LBL-15483
c.2

Lawrence Berkeley Laboratory
UNIVERSITY OF CALIFORNIA

THE REGENTS OF THE
LAWRENCE
BERKELEY LABORATORY
FEB 18 1983
LIBRARY AND
DOCUMENTS SECTION

Accelerator & Fusion Research Division

Presented at the NATO Advanced Study Institute on
Atomic and Molecular Processes in Controlled
Thermonuclear Fusion, Palermo, Italy,
July 19-30, 1982

NEUTRAL PARTICLE BEAM PRODUCTION AND INJECTION

D. Post and R. Pyle

July 1982

TWO-WEEK LOAN COPY
This is a Library Circulating Copy
which may be borrowed for two weeks.
For a personal retention copy, call
Tech. Info. Division, Ext. 6782.

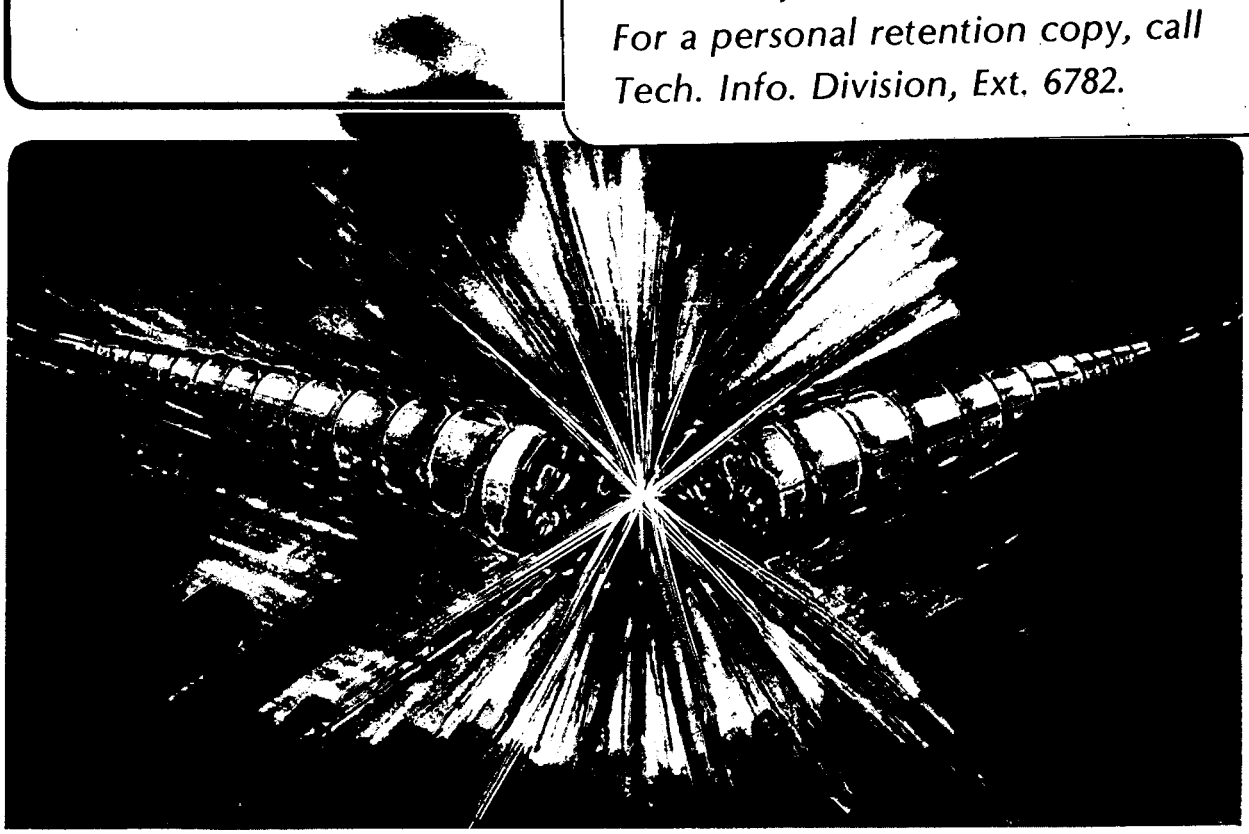

Prepared for the U.S. Department of Energy under Contract DE-AC03-76SF00098

LBL-15483
c.2

DISCLAIMER

This document was prepared as an account of work sponsored by the United States Government. While this document is believed to contain correct information, neither the United States Government nor any agency thereof, nor the Regents of the University of California, nor any of their employees, makes any warranty, express or implied, or assumes any legal responsibility for the accuracy, completeness, or usefulness of any information, apparatus, product, or process disclosed, or represents that its use would not infringe privately owned rights. Reference herein to any specific commercial product, process, or service by its trade name, trademark, manufacturer, or otherwise, does not necessarily constitute or imply its endorsement, recommendation, or favoring by the United States Government or any agency thereof, or the Regents of the University of California. The views and opinions of authors expressed herein do not necessarily state or reflect those of the United States Government or any agency thereof or the Regents of the University of California.

NEUTRAL PARTICLE BEAM PRODUCTION AND INJECTION*

D. Post
Princeton Plasma Physics Laboratory

R. Pyle
Lawrence Berkeley Laboratory,
University of California,
Berkeley, CA 94720

INTRODUCTION

Intense neutral beams are used to heat, fuel, adjust electric potentials, and diagnose fusion plasmas. They may be used to sustain currents in plasmas. We shall comment on some of the ways that atomic physics enters into the design, diagnosis, and application of neutral beam systems. It will be apparent that the treatment is selective and superficial, but we hope to mention most areas of interest, and indicate that there is a continuing need for new ideas and new techniques.

This paper is divided into two sections: The first is a discussion of the interactions of neutral beams with confined plasmas, the second is concerned with the production and diagnosis of the neutral beams. In general we are dealing with atoms, molecules, and ions of the isotopes of hydrogen, but some heavier elements (for example, oxygen) will be mentioned. The emphasis will be on single-particle collisions; selected atomic processes on surfaces will be included.

The two chief plasma physics requirements that a fusion reactor must meet are adequate confinement and a temperature of

* This work was supported by in part by the Director, Office of Energy Research, Office of Fusion Energy, Development and Technology Division, of the U.S. Department of Energy under Contract No. DE-AC03-76-SF00098, and in part by PPPL DOE Contract No. DE-AC02-76-CH03073.

about 10 keV or greater. The requirements for confinement ($n\tau_E > 10^{14}$ sec/cm^3, where n is the plasma density and τ_E is the confinement time) occurs because the energy loss rate of the plasma cannot exceed the self heating rate by alpha particles produced by DT fusion in a fusion reactor.[1] The second requirement of a temperature of 10 keV occurs because the D-T (deuterium-tritium) fusion reaction rate is small for temperatures below 10 keV.[2] A D-D (deuterium-deuterium) reactor would require temperatures of 30 keV or more. The issues of interest to fusion research are thus not only of plasma confinement but plasma heating. A typical reactor would be heated in steady state by the slowing down of the 3.5 MeV alpha particles produced in the fusion reaction. However, the plasma will have to be heated to the 10 keV, or so, at which the plasma heating is significant and, of course, present experiments need to be heated. Neutral injection has been the most successful heating method to date in magnetic fusion research.

Tokamaks require a toroidal current for confinement and equilibrium. This current is usually supplied by a change of flux in a coil. The need for the flux swing in the transformer coils sets a time limit on the tokamak pulse of about 10^3 - 10^4 seconds for a reactor. Then the tokamak plasma must be terminated and the flux reversed in the current driving coil. The termination and restarting of the plasma burn introduces thermal cycling stresses in the structure of the reactor, increasing the design requirements. There is thus great interest in a "steady state" tokamak in which the current is driven by a means other than by transformer action by a flux swing in a coil. Neutral beams can inject momentum into the plasma, and have been proposed for current drive in tokamaks.[3]

Experiments and reactor designs based on the mirror concept [4,5] require a large high energy population of ions with relatively low velocities parallel to the magnetic field. The high energy of the ions is necessary to maintain a large electrostatic field for electron confinement. In most current mirror experiments and reactor designs, this population of ions with $v_\parallel / v_\perp$ small is provided by neutral injection.

A typical neutral injection system involves an ion source, an acceleration system, a neutralization system, and a beamline to connect to the torus (Fig. 1). The energetic neutral atoms cross the magnetic field that confines the plasma, and are captured in the plasma by electron and ion impact ionization and charge exchange. The captured fast ions slow down, gradually heating the plasma by elastic coulomb collisions with the plasma ions and electrons. If energetic deuterons are injected into a plasma containing tritium ions, some of the deuterons can undergo fusion reactions with the tritons as they slow down.

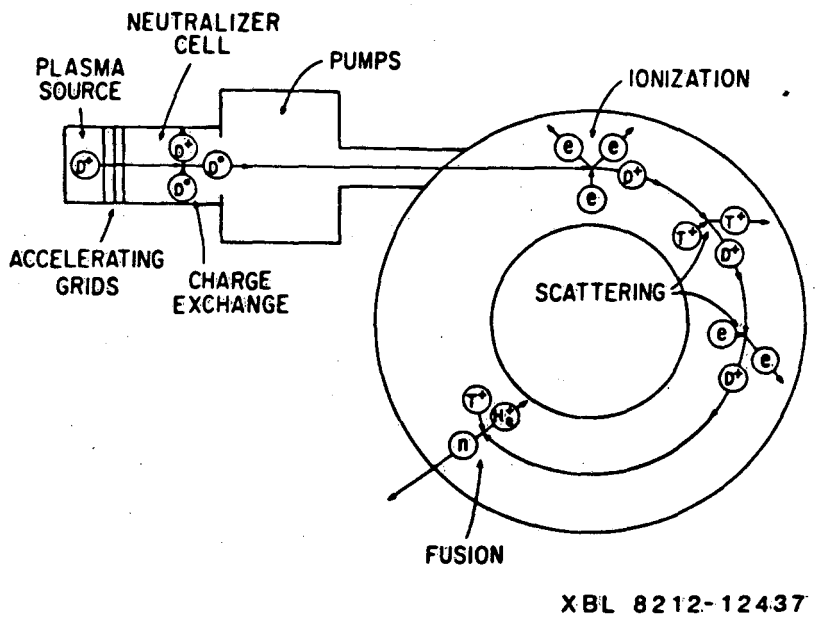

Fig. 1. Neutral injection by the acceleration of H^+ and neutralization by charge exchange, and the subsequent stopping of the beam in the plasma by coulomb scattering and nuclear reactions. (taken from Ref. 6)

The fast ions from the injected beam often have large orbits which must be confined. In addition, lack of axisymmetry due to the discrete toroidal field coils in the tokamak or the inherent lack of symmetry in the magnetic field topology of a mirror or stellerator can lead to unconfined orbits.[6] This loss mechanism for beam ions is not expected to be severe for large, high current tokamaks, but these losses are an area of active research for stellerators.[7]

The injection of neutral hydrogen atoms can enhance the impurity radiation in plasma experiments through such reactions as[8]

$$C^{+6} + H^{o} \rightarrow C^{+5}$$
$$C^{+5} + e^{-} \rightarrow (C^{+5})^{*} \rightarrow C^{+5} + h\nu$$

The hydrogen atoms enhance the recombination rate of the carbon (or other impurity ions). The recombined ions can then be excited by electron impact with background electrons, often leading to an increase in the impurity radiation losses in the fusion experiment.

Present neutral injection systems are based on positive ions. The low neutralization efficiency of such ions at energies above ~ 80 keV/amu limits the usefulness of positive

ion systems.[9] Future large tokomaks and mirror experiments would profit from the use of high energy beams with energies above 100 keV/amu. Such beams would be based on negative ions which can be neutralized efficiently. The use of negative ions also opens up the option of using neutral beams of elements heavier than hydrogen at extremely high energies (10-20 MeV).

NEUTRAL BEAM PENETRATION AND FAST ION ORBITS

Neutral injection systems are designed to produce a well collimated beam of neutral hydrogen atoms. The neutral atoms freely cross the confining magnetic field where they are captured by charge exchange and ionization[10] (Fig. 2) the attenuation along the beam is then given by

$$I = I_0 \exp(-n_e \sigma_{eff} x) = I_0 \exp(-x/\lambda).$$

This attenuation is averaged over each flux surface to produce a source of hot ions for each flux surface.[11,12] The local beam deposition rate, normalized by the volume averaged beam deposition rate, is defined as H(r). H(r) > 1 implies greater than average local heating (Fig. 3).

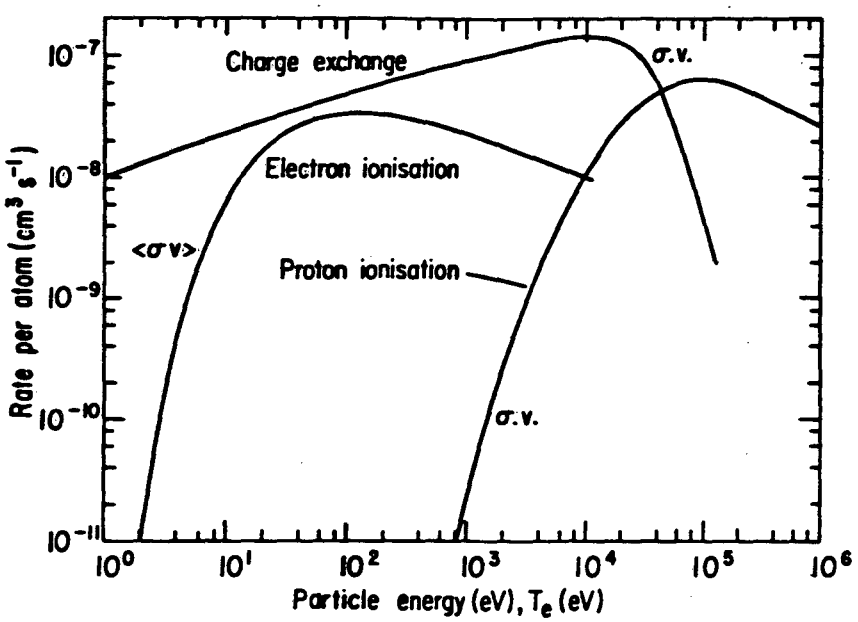

XBL 8212-12438

Fig. 2. Reaction rates for atomic hydrogen for electron impact ionization, proton impact ionization, and charge exchange with protons as a function of lab hydrogen energy. The energy scale for the electron ionization rate is the electron temperature.

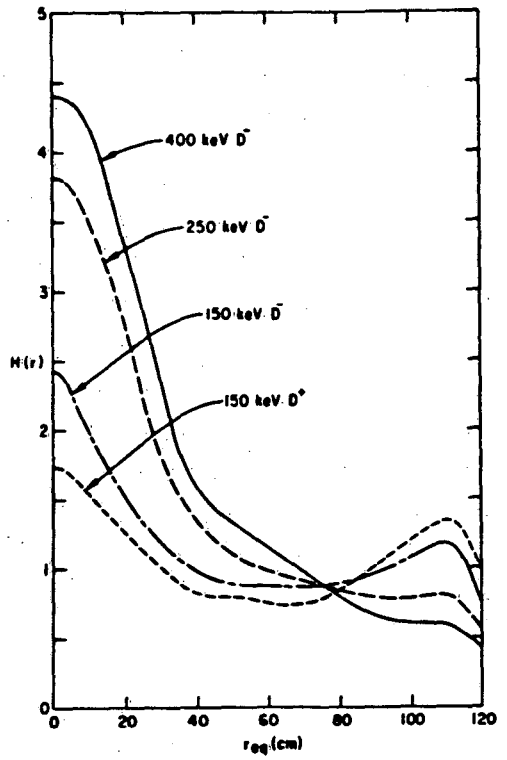

Fig. 3. Neutral beam deposition profiles for 150, 250, and 400 keV D^- based beams and for a 150 keV D^+ based beam on small version of the proposed FED tokamak.[13]

The presence of impurities can affect the ionization of the injected beam. The two processes of interest are charge exchange and ion-impact ionization of H_o with multiply-ionized impurity ions[14]

$$A^{+q} + H^o \rightarrow A^{+q} + H^+ + e^-$$
$$\rightarrow A^{+q-1} + H^+.$$

An enormous amount of theoretical and experimental work has gone into determining these cross sections.[15] It was expected that the dominant process might be ion impact ionization which would scale as Z^2. Thus the cross section for beam penetration would scale as $Z_{eff} = \frac{n_H + Z^2 n_Z}{n_e}$ where n_H is the hydrogen density, n_Z is the impurity density and n_e is the electron density. Typical plasmas often have $Z_{eff} \sim 2 - 5$. A mean free path that scaled as $\lambda = \lambda_H/Z_{eff}$ would preclude heating of most plasma experiments by neutral beams since the beam ions would all be deposited on the plasma edge.

Fortunately, it turned out that the dominant process at the energies of interest is charge exchange, which scales more like Z than Z^2. Thus we have

$$\frac{1}{\lambda} = n_e \sigma_{eff} = n_H \sigma_{ion} + n_H \sigma_{cx} + \frac{n_e \langle \sigma v \rangle_e}{v_b} + \sum_Z n_i (\sigma_{Zion} + \sigma_{Zcx})$$

where σ_{ion} is the hydrogen ion impact ionization cross section, σ_{cx} is the hydrogen charge exchange cross section, $\langle\sigma v\rangle_e$ is the electron impact ionization cross section, and the last term represents the impurity ionization and charge exchange cross sections. Noting that $\sigma_{Zcx} \sim Z\sigma_H$, we have approximately, in the range where $\sigma_{cx} << \sigma_{ion}$,

$$n_e \sigma_{eff} = n_H \sigma_{ion} + \frac{n_e \langle\sigma v\rangle_e}{v_b} + n_Z Z \sigma_{ion}$$

$$= (n_H + Z n) \sigma_{ion} + \frac{n_e \langle\sigma\rangle_e}{v_b}$$

$$= n_e (\sigma_{ion} + \frac{\langle\sigma v\rangle_e}{v_b}) .$$

Thus by ignoring the impurities and treating the plasma as a pure hydrogen plasma, we would have obtained almost the right answer (Fig. 4). Nonetheless, it was crucial that the question be resolved as the fusion community was spending ~ \$2 x 10^9 on TFTR, JT-60 and JET, and these experiments would not work well with beam injection if the penetration cross section scaled as Z_{eff}. At high injection energies of 300-1000 keV and higher, the dominant process is ion impact ionization which does scale as Z^2, so this process will be important for high energy beams.

An approximate formula for the trapping length in a large tokamak has been worked out by the INTOR group[16] for a deuterium beam:

$$\lambda = 2.8 \times 10^{13} \frac{E_b \text{ (KeV)}}{n_e \text{ (cm}^{-3})} \text{ cm.}$$

For perpendicular injection, $\lambda \sim a/2$, where a is the plasma minor radius, ensures reasonable beam penetration. This implies that the injection energy should scale as

$$E_b(\text{KeV}) = 180 \times 10^{-16} \text{ na},$$

yielding an energy of ~ 300 KeV for INTOR parameters.[17] The good penetration requirement can be ameliorated by initially injecting into a low density plasma and gradually building up the plasma density as the alpha heating increases, and by the shift outward of the flux surfaces as the plasma heats up, which

reduces the column density of plasma to the plasma center.[18]

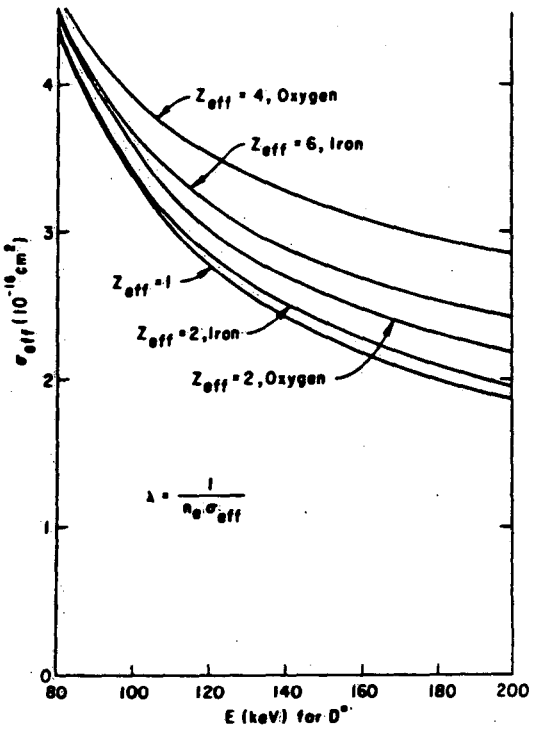

XBL 8212-12440

Fig. 4. Effective trapping cross section versus neutral hydrogen beam energy, defined as:

$$\sigma_{eff} = \frac{Z-Z_{eff}}{Z-1}\left(\sigma^{H}_{cx} + \sigma^{H}_{p\text{-}ion}\right) + \frac{Z_{eff}-1}{Z(Z-1)}\left(\sigma^{imp}_{cx} + \sigma^{imp}_{ion}\right) + \frac{\langle\sigma v\rangle_{e\text{-}ion}}{v_{beam}}$$

for a deuterium neutral beam traversing a deuterium plasma with an impurity of charge Z. σ^{H}_{cx} is the hydrogen charge exchange cross section, σ^{H}_{p}-ion is the proton impact ionization cross section, σ^{H}_{cx} is the impurity-hydrogen charge exchange cross section and σ^{H}_{ion} is the ion impact ionization cross section.[10,13]

However, a high beam energy is still desirable as it makes heating the plasma center less problematical.

As can be seen from above, the mean free path is roughly proportional to the beam energy. The presence of hydrogen atoms with one-half and one-third of the acceleration potential in the beams, formed from H_2^+ and H_3^+ in the ion source, greatly reduces the heating effectiveness of the beam.

Mirror plasmas are usually sufficiently small that penetration is not a problem. In fact, in a number of reactor designs,

only 10-20% of the beam is ionized by the plasma. The upper limit on the beam energy is often set in such designs by this requirement.

Fast ions in a tokamak often have large orbits. If the tokamak is completely axisymmetric, then the toroidal angular momentum of the ions is conserved:[19]

$$P_\phi = mv_\phi R + (ZeR/c) A_\phi = \text{constant},$$

where R is the major radius, v_ϕ is the velocity around the torus, m is the mass of the beam ion, Z is the charge of the beam ion, and A_ϕ is the vector potential around the torus due primarily to the plasma current. The conservation of P_ϕ implies that the orbits are periodic and thus, if the beam particles don't hit the wall or limiter, they are confined. The angular momentum of the ions as they gyrate about the field lines is also conserved. This implies that the magnetic moment of the particles is conserved as the magnetic field strength is varied along a field line since $M\, v_\perp \rho_L$ = constant together with the gyroradius $\rho_L = \frac{v_\perp}{eB/mc}$ implies that $\frac{mv_\perp^2}{2B} = \mu$, a constant, where μ is the magnetic moment of the particle and $v_\perp$ is the component of the velocity of the particle perpendicular to the field line.

The conservation of μ implies for particles of a given $v_\perp$ and total velocity v, there is an upper limit to the magnetic field strength for their orbits. Writing,

$\varepsilon = \frac{1}{2} m(v_\parallel^2 + v_\perp^2)$ and substituting μ for $v_\perp^2$, we see that

$v_\parallel = [2(\varepsilon - \mu B)/m]^{1/2}$,

and that for a constant ε and μ, there is maximum B at which $v_\parallel = 0$ and above which v is imaginary. Thus these particles are reflected from regions of high field strength toward regions of lower field strength along a field line. This is the basis for confinement in the mirror concept[4].

Since the magnetic field obeys Ampere's law, $\nabla \times B = 4\pi/c\, j$, a toroidal magnetic field falls off as 1/R, where R is the distance from the center line of the torus. (BR = constant). We can approximate $R = R_0 (1 + r \cos \theta)$, where R_0 is the major radius of the magnetic axis of the torus, r is the minor radius, and θ is the angle r makes with toroidal plane (Fig. 5). Conservation of magnetic moment implies

$$\frac{mv_\perp^2}{2} = \mu B_T = \mu B_o \frac{R_o}{R} = \mu B_o \left(1 - \frac{r}{R_o} \cos \theta\right).$$

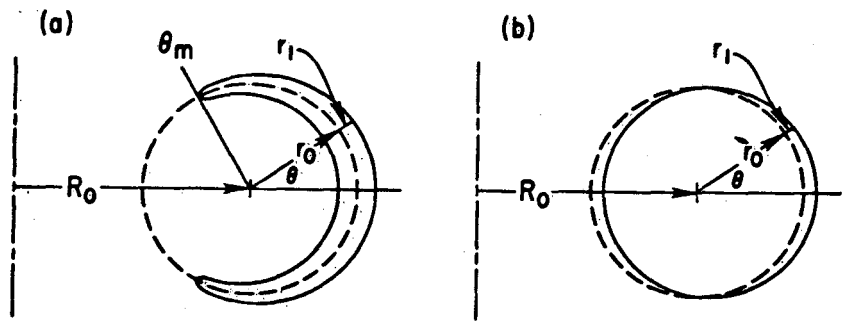

XBL 8212-12441

Fig. 5 (a). Particles with $\left(\frac{V_\parallel}{V_\perp}\right)^2 < 2r/R$ at $\theta=0$ are trapped and their guiding centers make banana shaped trajectories about the flux surfaces.

5 (b). Particles with $\left(\frac{V_\parallel}{V_\perp}\right)^2 > 2\frac{r}{R}$ at $\theta=0$ are not trapped, "passing," and have orbits that are shifted depending on the sign of V . Taken from Ref. 6.

As θ increases toward $\pm\pi$ (Fig. 5) R decreases and B increases, so that beam ions with

$$\frac{v_\parallel^2}{v_\perp^2} \leq 2r/R_o \text{ at } \theta = 0$$

are trapped (as in a mirror) on the large R side of the plasma (Fig. 5), similar to the particles in the Van Allen belt.[4] Tangentially injected beam ions ($v_\perp << v_\parallel$) will execute orbits which are circles with centers displaced by a distance Δ from the magnetic axis (Fig. 6).[6]

The consequences of these shifts is that all of the coinjected (injected parallel to the plasma current) beam ions deposited outside the region of width 2Δ are confined. This is usually the case. In contrast, all of the counter-injected beam ions deposited in the outside region of width 2Δ are lost. The lost fast ions often sputter limiter and wall material with the result that the observed impurity levels in discharges with counter injection are often higher than with co-injection.

In order to achieve better penetration with a given energy beam, the beam is often oriented perpendicular to the torus to minimize the distance to the magnetic axis. Then the fast ions have $v_\perp >> v_\parallel$ and have trapped (Fig. 5a) orbits. Unless the plasma current is large many of the ions captured near the plasma edge can scatter (due to collisions with plasma ions) into orbits that intersect the limiter and are lost.

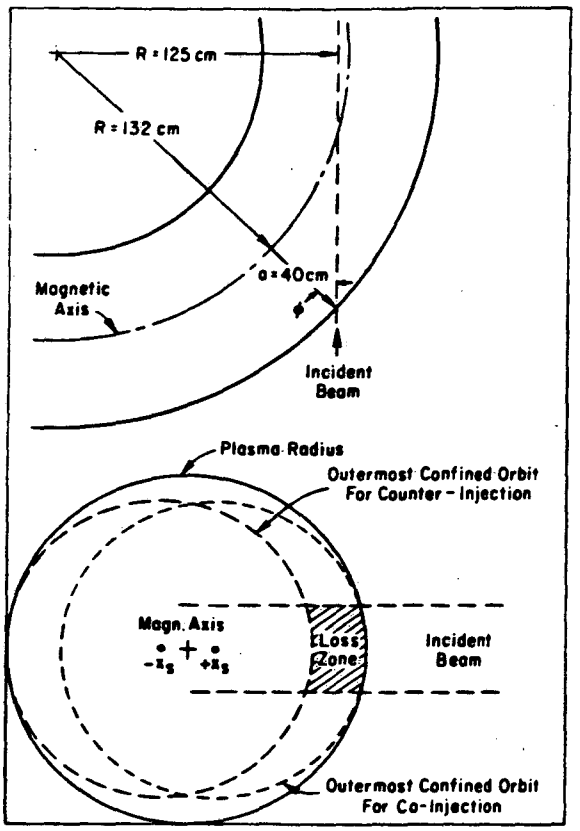

XBL 8212-12442

Fig. 6. Schematic of neutral injection on PLT. All of the counter injected ions that are captured in the shaded region have orbits that intersect the wall of limiter and are lost. Taken from Ref. 6.

One problem with perpendicular injection arises from the fact that the toroidal field in tokamaks is produced with discrete coils. The toroidal field "bulges out" slightly between coils with the result that the field strength varies along a field line and the field is not axisymmetric. The loss of axisymmetry implies that the canonical angular momentum around the torus is not conserved and the particle orbits are not necessarily periodic. Ions may be locally trapped between two coils in local minima in the field or scatter off the irregularities in the field and eventually drift out of the plasma (Fig. 7). Perpendicular

injection produces initially trapped ions which can be strongly affected by the ripple.

Injection into inherently non-axisymmetric systems such as stellarators, mirrors, and bumpy toruses suffers from many of the same problems as rippled tokamaks. Nonetheless, neutral injection is being used successfully on stellarators and mirrors.

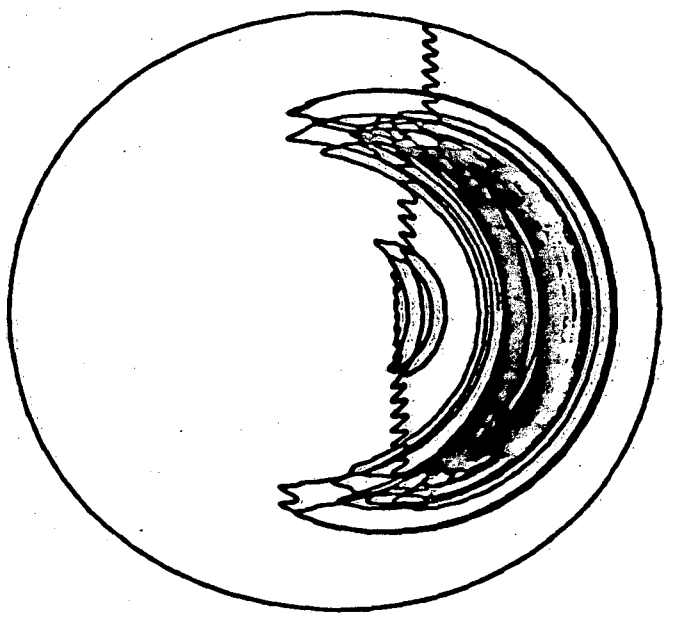

XBL 8212-12435

Fig. 7. A trapped ion injected near perpendicularly into a 30 cm plasma with a 3% field ripple is easily trapped and detrapped in local magnetic mirrors by small angle scattering due to collisions with the ions and escapes by vertical drift. (Taken from Ref. 6, originally calculated by R. Goldston).

FAST ION SLOWING DOWN AND PLASMA HEATING

The fast ions from neutral injection slow down by elastic coulomb collisions with the background ions and electrons. The rate at which a typical fast ion of energy E_f, charge Z_f and atomic number A_f slows down in a plasma composed of ions of atomic number A_i and charge Z_i, and electron temperature T_e, is given by[20]

$$\frac{dE_f}{dt} = -\frac{\alpha}{(E_f)^{1/2}} - \beta E_f = -\beta\left(E_f + \frac{E_c^{3/2}}{E_f^{1/2}}\right)$$

where the alpha term represents slowing down due to collisions with the ions and the beta term represents slowing down due to collisions with the electrons. α and β are defined as:

$$\alpha = 4\pi e^4 \ln \Lambda_i \left(\frac{A_f}{2m_p}\right)^{1/2} Z_f^2 \sum_i \frac{Z_i^2 n_i}{A_i}$$

and

$$\beta = \frac{8}{3} (2\pi m_e)^{1/2} \frac{e^4 \ln\Lambda_e n_e Z_f^2}{(KT_e)^{3/2} m_p A_f} .$$

The critical energy E_c, is defined as the beam energy at which beam heating of electrons and ions is equal:

$$E_c = (\alpha/\beta)^{2/3} = 14.8 A_f kT_e \left[\Sigma \frac{(\ln \Lambda_i) Z_i^2 n_i}{(\ln \Lambda_e) A_i n_e}\right]^{2/3} .$$

When $E_f > E_c$ the electron heating is greater, and when $E_f < E_c$, the instaneous ion heating is greater. The two coulomb logorithms are

$$\ln \Lambda_e = 23.9 + \ln (Te\ (eV)/ (n_e\ (cm^{-3}))^{1/2})$$

and

$$\ln \Lambda_i = -5.2 + \ln \left(\left(\frac{T_e\ (eV}{n_e\ (cm^{-3})}\right)^{1/2} \frac{v_f^2\ cm/sec\ A_f A_i}{Z_f Z_i (A_f + A_i)}\right) .$$

For typical tokamak reactor conditions with $n = 10^{14}$ cm^{-3}, $T_e = 10^4$ eV, and 120 KeV D^o injection, $\ln \Lambda_i = 22.7$, and $\ln \Lambda_e = 17$.

The thermalization time is defined as the time it takes an ion to slow down from the initial energy E_o to 0.

$$\tau_{Th} = - \int_{E_o}^{o} \left(\frac{dE_f}{dt}\right) dt = \frac{\tau_s}{3} \ln \left(1 + \left(\frac{E_o}{E_c}\right)^{3/2}\right)$$

where τ_s is a slowing down time for the electrons defined as

$$\tau_s = \frac{2}{\beta} = .371 \frac{A_f}{Z_f^2} \left(\frac{T_e}{10\ \text{KeV}}\right)^{3/2} \left(\frac{10^{14}}{n_e}\right) \left(\frac{17}{\ln \Lambda_e}\right) \text{sec}$$

and E_0 is the injection energy. Typical thermalization times in present day experiments are .015 - .030 seconds, primarily due to the low T_e [Table 1].

Table 1. Beam and injection parameters of the PLT AND TFTR experiments (Z_{eff} = 2).

	PLT	TFTR	TFTR	TFTR
Beams	40 KeV H	120 KeV D	120 KeV D	3.5 MeV α particles
n	5×10^{13} cm	5×10^{13} cm	10^{14} cm	10^{14} cm
T	2 KeV	5 KeV	10 KeV	10 KeV
τ_s	.066 sec	.52 sec	.74 sec	.37 sec
E_c	42 KeV	210 KeV	220 KeV	470 KeV
Th	.015 sec	.062 sec	.084 sec	.377 sec

For the next generation of tokamak fusion experiments such as TFTR, the thermalization times are roughly .06 seconds, while 3.5 MeV alpha particles in TFTR will have thermalization times of roughly .4 seconds. The alpha particles will primarily heat the electrons ($E_\alpha \gg E_{crit}$) whereas the fast beam ions will primarily heat the plasma ions.

Neutral beams are used for heating on PLT, PDX, ISX, D-III, TFR, ASDEX, DITE, JFT-2, JIPPT-II, and T-11.[6] On PLT the ion temperature was heated to approximately 7 KeV with 2.5 MW of D^0 neutral beams injected into a hydrogen plasma[2] (Fig. 8). TFTR, JET and JT-60 will all use neutral beams.

TFTR[6] is designed to take advantage of the fact that the DT fusion cross section peaks between 100 KeV and 200 KeV. Thus, 120 KeV deuterium beam ions have a significant probability of reacting with the tritium ions while they are slowing down. Most of the contribution to the fusion reaction rate comes from the high energy tail (near 100 KeV) of the Maxwell-Boltzman distribution, and with 120 KeV D^0 neutral injection, all of the beam ions are injected at near the optimum velocity for fusion. Taking advantage of the reacting beams, scientific break-even (defined as the condition where the fusion power

produced in the plasma is comparable to the heating power can be achieved with $n\tau_E \sim 10^{13}$ sec/cm^3 instead of the more severe requirement that $n\tau_E \sim 10^{14}$ sec/cm^3 when the fusion power must be produced by thermonuclear reactions[22].

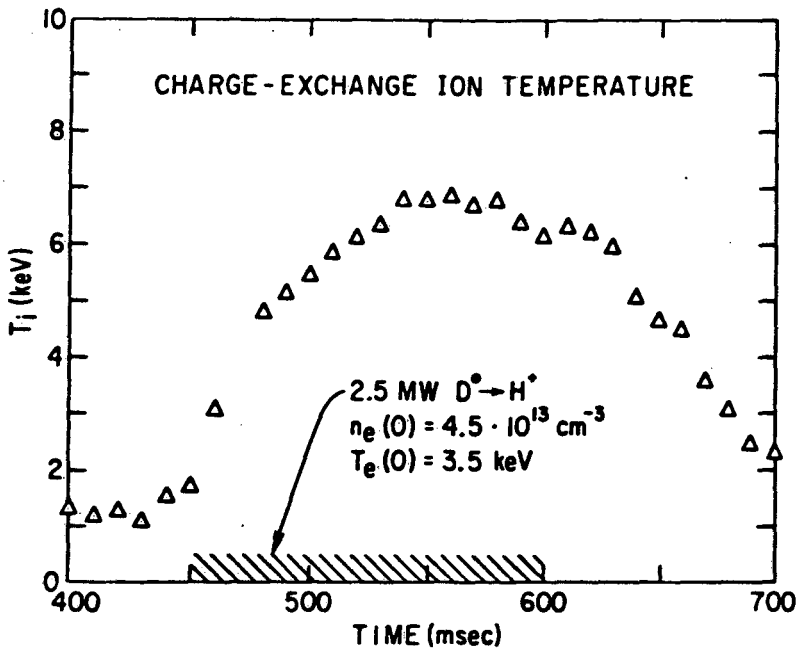

XBL 8212-12436

Fig. 8. Charge-exchange ion temperature in PLT for the injection of 2.5 MW D^0 beams into an H^+ plasma, measured by a mass selective (H^+) fast neutral detector. (Taken from Refs. 6,21).

Neutral beams are a crucial part of producing confined particles in mirror experiments[4]. As we have seen, particles with small enough $v_\parallel/v$ at the center low field region are confined. From conservation of energy and magnetic moment one can show that particles with pitch angles $\xi_c = \frac{v_\parallel}{v} < \sqrt{1 - B_c/B_m}$ are confined, where B_c is the field at the low field central point along the field line at which ξ_c is determined and B_m is maximum field along the field line. Particles with larger ξ_c are unconfined since $v_\parallel$ never goes to zero. Thus a mirror confined plasma consists of particles with $v_\parallel/v < \xi_c$. Collisions which change the pitch angle can change the particle from confined to unconfined. Thus the particles are confined for a collision time. The ion and electron collision times for 90° changes in the pitch angle are given below.

$$\tau_{ii} = \frac{2 \times 10^{11} \sqrt{M}}{n \ln\Lambda \; Z_1^2 \; Z_2^2} E_i^{3/2} \text{ sec}$$

and

$$\tau_{ee} = \frac{10^{10}}{n \ln\Lambda} T_e^{3/2} \text{ sec}$$

where $Z = q/e$ and M is the ion mass in atomic units; E_i is the ion energy in keV; T_e is the electron temperature in keV. For $T_e \lesssim E_i$, as is the usual case for beam heated mirrors, $\tau_{ee} \ll \tau_{ii}$, and the electrons quickly become unconfined. The electrons thus would leak out of the mirror much more quickly than the ions except that the positive charge of the ions holds the electrons back. Thus a positive potential, ϕ, forms which holds the electrons back (confining them electrostatically) so that the ion and electron loss rates are equal. The electrons have to be confined for many electron collision times which requires the electrostatic potential $e\phi \gg T_e$. However $e\phi$ must be less than the ion energy E_i if the ions are to be confined so one must have $T_e \ll e\phi < E_i$. Since the ions are hotter than the electrons, the ions slow down and heat the electrons by collisions. The fast ions thus must be heated continuously, usually with neutral beams. Taking all of these effects into account[4], we find that for mirror machines the $n\tau$ (product of density and energy confinement time) is given by[4]

$$n\tau = 2.6 \times 10^{10} E_o^{3/2} \log_{10} (B_m/B_c) \text{ sec/cm}^3$$

where E_o is the injected neutral beam energy in keV. Thus high energy neutral beams are useful for good confinement in mirrors. The ions could also be heated by radiofrequency methods and preliminary experimental work on this has begun[4,5].

CHARGE EXCHANGE RECOMBINATION

In Section II, we saw that the reaction

$$A^{+q} + H^o \rightarrow A^{+q-1} + H^+$$

where A^{+q} is an impurity of charge q, had cross sections of ~ $Z^{1.2} \times 1.4 \times 10^{-16}$ cm^2. While this cross section was not large enough to greatly alter the neutral beam penetration situation, the cross section for this charge exchange could still be 10^{-15} to 10^{-14} cm^2. This charge exchange is an additional recombination mechanism for the impurity ions which can alter the charge state distribution of the impurities.

Since the impurities would be more recombined, and have more electrons to excite than would be the case without charge exchange recombination, the total impurity radiation could be increased by the injection of neutral beams into a plasma containing some impurities.[8]

A convenient way of parameterizing the effect is in terms of the ratio of the neutral density to the electron density. In coronal equilibrium, the relative abundance of adjacent ionization states is determined by the ratio of their total ionization and recombination rates[8]

$$\frac{n_{q-1}}{n_q} = \frac{R_q}{I_{q-1}} = \frac{\alpha_q^{Rad} + \sigma_q^{Die} + (n_o/n_e)\,\alpha_q^{cx}}{K_{q-1}}$$

where α_q^{Rad} is the radiative recombination rate coefficient, α_q^{Die} is the dielectronic recombination rate coefficient, K_q is the electron ionization rate, and

$$\alpha_q^{cx} = \sigma_{cx}^{q}\, v_{beam} \,.$$

Thus the usual coronal equilibrium charge state distribution and radiation losses are modified (Fig.9). Very little of the radiation enhancement comes from the charge exchange event and the subsequent radiative decay. Most of the radiation comes from subsequent electron excitation and radiative decay of the recombined ions.

This radiation has been observed on several tokamaks.[23,24] For the most practical situations, the increase in the impurity radiation caused by charge exchange recombination during neutral beam injection is only a small fraction of the beam heating power.

However, in DITE the increase in the radiative losses was as large as the beam heating power, resulting in no heating with the beam.[25] Fortunately, DITE had somewhat atypical conditions compared to most other beam injected tokamaks. The beam energy was low, decreasing v_o and therefore increasing n_o, the neutral density. DITE also had relatively high impurity levels, especially C, O and Ti. The radiation in DITE was also observed to be toroidal assymetric. The radiation rate near the beam was as much as a factor of 3 or more higher than the radiation 180° around the torus from the beam. Detailed modeling[25] showed that this was consistent with charge exchange recombination in the beam line of sight and subsequent

ionization as the impurity ions diffused along the field lines away from the beam.

Although charge exchange recombination enhanced radiation is not a major part of the power balance in most beam heated tokamaks, it can be important if the conditions are right (low n_e, high n_0, high impurity concentrations). The process also affects the spectroscopically observed charge state distribution, and must be included when using the observed

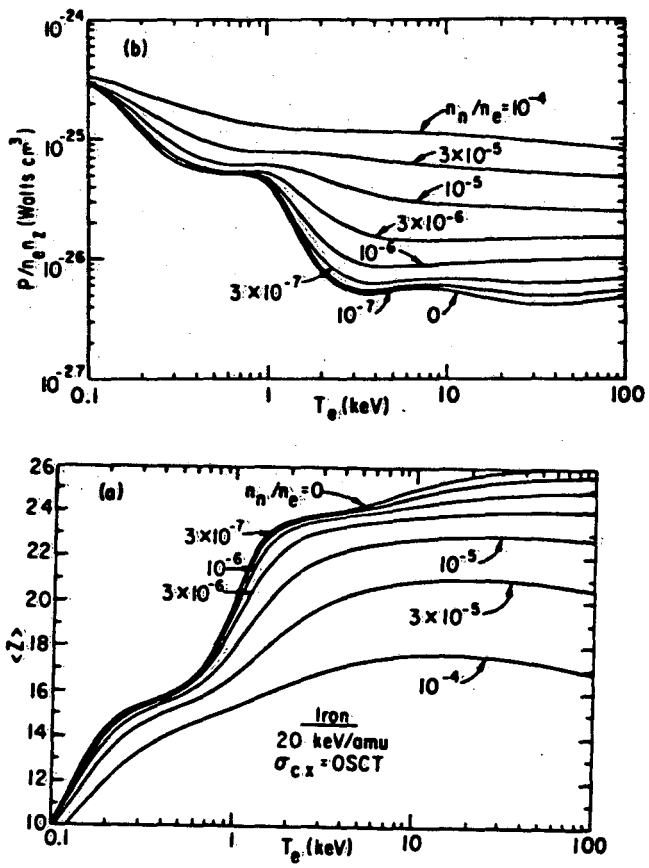

XBL 8212-12443

Fig. 9. Neutral beam modified coronal equilibria for iron. The beam energy is 20 keV/AMU. The curves are parametrized by the neutral fraction n_0/n_e. Shown are the average charge state <Z>, and (b) the overall radiation rate coefficient $P/n_e n_z$, both as functions of the electron temperature. (Taken from Ref. 8).

charge state distributions to determine the effects of beam injection on impurity transport.

CURRENT DRIVE AND HIGH ENERGY BEAMS

It is becoming a common perception that if tokamaks are to be seriously considered for fusion reactor designs, they must be steady state. The thermal cycling stresses produced when the tokamak must shut down and start up again cause enormous engineering problems. Thus a method for driving the current in a tokamak, or any other concept which relies on induced internal currents such as spheromaks, reversed field pinches and reversed field mirrors, would enhance the reactor prospects of that fusion containment approach.

Tangentially injected neutral beams form a circulating ion current [3]

$$j_{circ} = \frac{n_b \langle v_{\parallel} \rangle e Z_B}{2\pi R_o},$$

where j_{circ} is the local current density of fast ions, n_b is the density of beam ions, $\langle v_{\parallel} \rangle$ is their average parallel velocity, Z_B is the charge of the beam ions, and R_o is the major radius of the torus. The directed flow of the fast ions will try to drag the electrons along through coulomb collisions. In the absence of collisions, this electron current would cancel the ion current.

However, the electrons will slow down due to collisions with the background plasma. For the classical case, the friction of the beam ions on the electrons will equal the friction of the electrons on the background plasma for $Z_B = Z_{eff}$. The inclusion of trapped electrons (which cannot circulate toroidally as easily as the passing electrons), leads to a reduction in the electron current which would imply that a current would be driven even if $Z_B = Z_{eff}$. The total beam driven current is then

$$j_b = j_{circ} \left(1 - Z_b/Z_{eff} \left(1 - G \left(Z_{eff}, E\right)\right)\right)$$

where G is the neoclassical correction which depends on Z_{eff} and $E = r/R_o$. G is usually ~ 1/2.[26]

This current has been observed on DITE.[27] Experimental verification is difficult since the experiment must be done for a skin time (time for the magnetic field to resistively diffuse through the plasma) and the typical skin times are long compared to the pulse length of most machines. Clear signs that neutral beams have injected momentum into the plasma have been observed. Rotation speeds of up to 1.2×10^7 cm/sec have been observed on PLT with co-injection[28] (Fig. 10).

The optimum conditions for neutral beam current drive in-

volve a complicated set of tradeoffs. However recent studies[26] indicate that the optimum beam energy for current drive in a reactor is ~ 1 MeV for D^0, with about 100 MW of injected power required.

Given the interest in good penetration and therefore high energy for heating and high energy for current drive, considerable effort is being spent on the development of negative ion based neutral beams that would have essentially the same plasma physics as positive ion based neutral beams.

Recently studies have been done of the advantages and feasibility of using either very high energy neutral beams of atoms with Z > 1 based on negative ions or on very high energy single

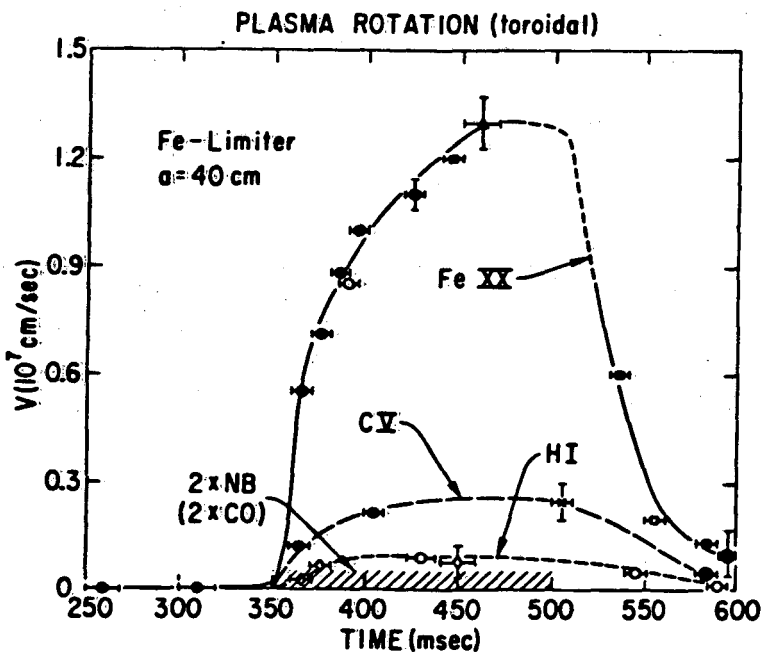

Fig. 10. The toroidal rotation velocity in PLT as a function of time for 1.5 MW of coinjected neutral beams (with an iron limiter). The different impurity ions and hydrogen light refer to different radial positions. (Taken from Ref. 28.)

ionized beams of such ions as B^+, Na^+, etc. for plasma heating.[29,30] The major advantage of these beams is that they would have a very high energy (~ 1 MeV/amu) and therefore would have very small currents for a given power compared to 100 KeV to 500 KeV neutral hydrogen beams (basically $1/Z^2$ less current and Z^2 higher energy for a given beam power).

The light atom neutral beam would penetrate into the plasma as a high energy neutral. Then the atom would be singly ionized, and begin to drift in the magnetic field. As the singly ionized ion was successively ionized to progressively higher charge states, the gyroradius would shrink ($\rho \propto 1/Z$), and the orbit would change. The excursions from the flux surface would also become smaller (Fig. 11). The combination of a penetration as a high energy neutral and as a drifting ion with a shrinking gyroradius can lead to very centrally peaked heating profiles.

The accurate computation of these orbits requires a knowledge of the ion impact ionization cross sections for the injected atoms at energies of ~ 1 MeV/amu. The computations (Fig. 11) were done using a semi-classical prescription[31] (Fig. 12). More accurate cross sections would be useful if they become available.

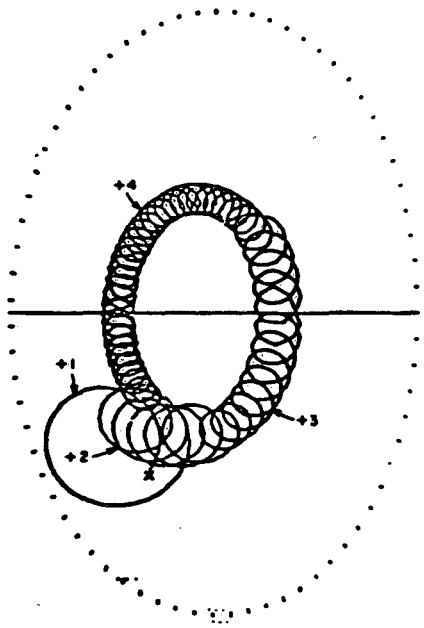

XBL 8212-12445

Fig. 11. A trajectory of a 32 MeV oxygen neutral atom injected into a larger plasma. The ion is progressively ionized as it drifts toward the plasma center. (Taken from Ref. 29).

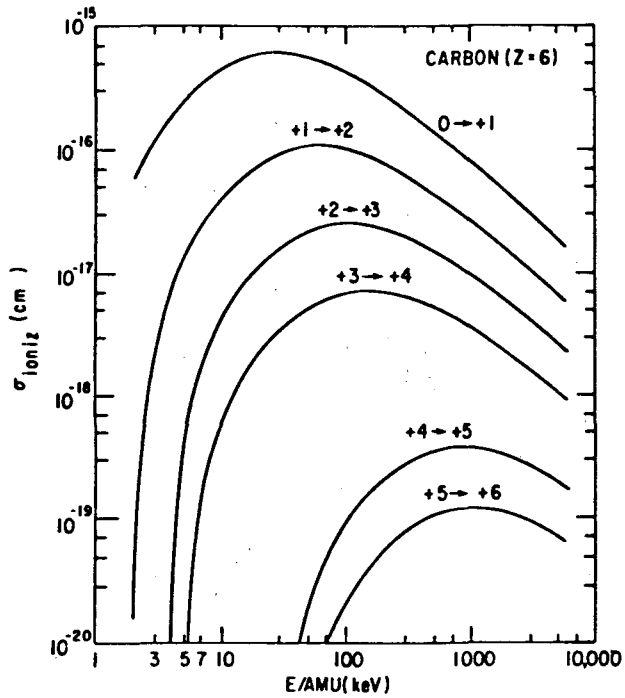

Fig. 12. Proton impact ionization cross sections for carbon as a function of the relative energy. (Taken from Ref. 29, based on Ref. 31).

NEUTRAL BEAM SYSTEMS

GENERAL PARAMETERS

The large fusion experiments that will operate during the 1980's require tens of megawatts of neutral hydrogen or deuterium beams with particle energies of about 40-80 keV/nucleon, and pulse lengths up to 30 seconds. These beams are obtained by charge exchange in low-pressure gases. Preliminary designs for future experiments and reactors use injection energies of more than 100 keV/nucleon; it is assumed that these beams will be obtained by collisional- or photo-detachment of electrons from intense, energetic beams of negative ions.

For a number of technical reasons neutral beam systems are built and operated as a number of separate modules. Typical parameters for a positive-ion module are: accelerated current ~ 40 - 100 A, active area (accelerator area) ~ 200 - 400 cm^2, accelerator transparency ~ 50%, current density at the plasma ~

0.2 - 0.5 A cm^{-2}. Details of two typical modules are given in references 32 and 33.

Positive-Ion Systems

An artists conception of the Princeton Plasma Physics Laboratory TFTR experiment with four neutral beam injection lines (three shown at the right) is given in Fig. 13.

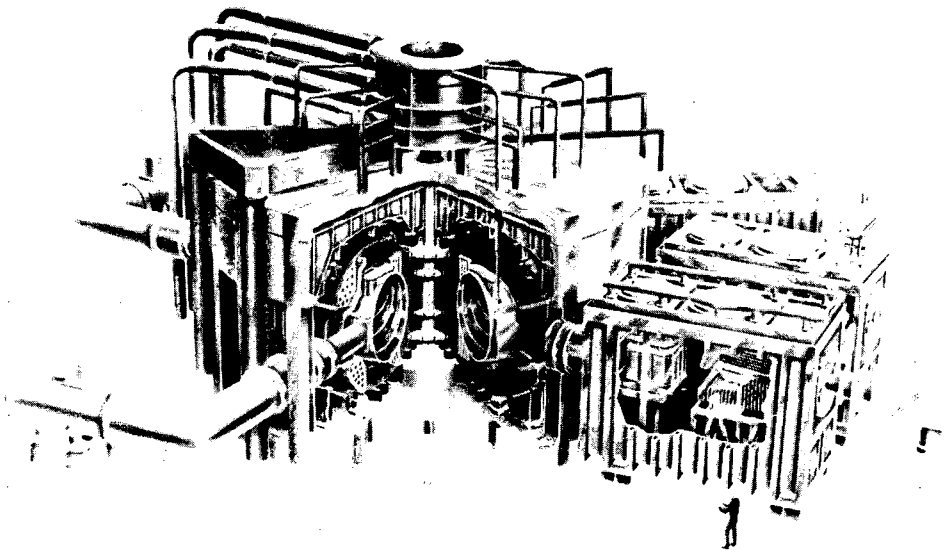

XBB 827-6076

Fig. 13. Artist's conception of the Princeton Plasma Physics Laboratory TFTR experiment.

Each of the neutral injection lines has three 120 kV, 65 A(power supply drain) plasma source/accelerator modules. Four beamlines (12 source modules) will inject about 20 MW (total) of 120 KeV D^0 atoms into the confined plasma.[34] The cost of such a system is several dollars per watt of neutral beam.

A system of this type, based on the production, acceleration, and neutralization of positive ions is shown schematically in Fig. 14. A moderately dense plasma ($n_i = n_e > 10^{12}$ cm^{-3}) is produced by a d.c. or r.f. discharge in a chamber containing hydrogen or deuterium at low pressure, typically 1-10 mtorr. Neither the energy distributions of the electrons, ion, atoms and molecules, nor the composition of this partially-ionized gas are known in detail. The bulk of the electrons have a temperature of a few electron volts, and there is a population with energies up to about 100 eV. The diassociation of the hydrogen in the discharge chamber is inferred from a model, and is very uncertain, perhaps 50%. The ion temperature is inferred

from the angular distribution of an accelerated beam, and is also subject to large uncertainties, but is less than one electron volt.

In addition to the atomic and molecular hydrogen ions, the plasma also contains impurities, especially oxygen, that may be accelerated and neutralized, and/or may affect the composition of the hydrogen plasma ($H^+:H_2^+:H_3^+$). Present plasma sources typically give ion beams which are about 1% oxygen, in the form of a water ion. This is unacceptably large for many planned experiments. There is little information about other contaminants.

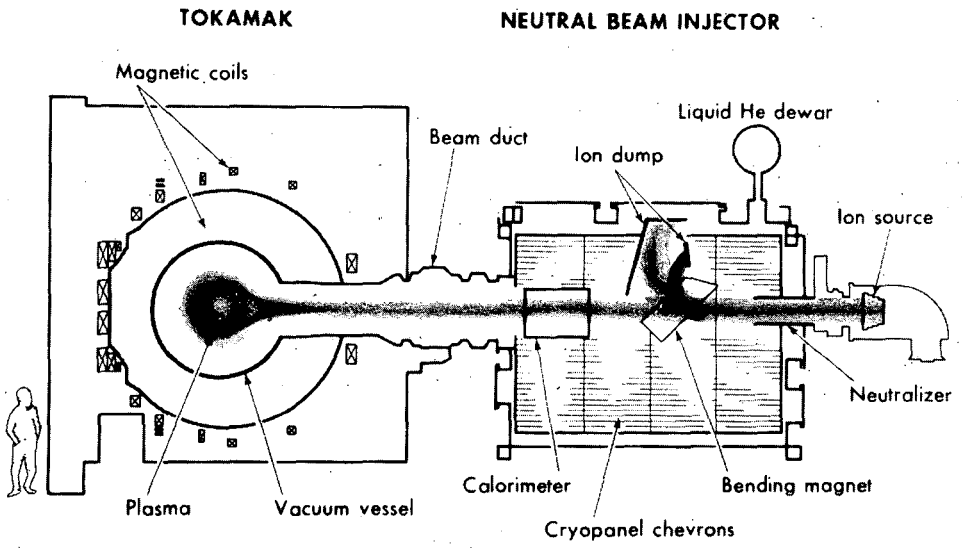

NEUTRAL BEAM INJECTOR AND THE TOKAMAK (TFTR)
CBB 826-5474

Fig. 14. Schematic of a positive-ion-based neutral beam line, from the viewpoint of the neutral beam developer.

Ions and electrons in the plasma eventually reach the walls of the discharge chamber. Attached to one of the walls is an accelerator structure containing three or four electrodes, each containing many slots or circular holes. The plasma generator and accelerator combine into a single module often called an "ion source". Ions and neutral gas from the plasma generator pass through the accelerator into the neutralizer. The neutralizer is a region one or two meters long, which contains hydrogen or deuterium gas at an average pressure of a few millitorr, i.e., the accelerated ions enter a region containing about 10^{16} molecules cm^{-2}, in which neutralization by electron capture can occur. Molecular ions also produce neutrals by collisional dissociation.

The remaining part of the neutral beam system, by far the largest and most expensive part, consists of components to separate the neutral and residual ion beams, cryogenic vacuum pumps, diagnostics, power supplies, and computers for data acquisition and control. A description of a complete system is given in Ref. 35. The required gas pumping-speed in a long-pulse system, such as is shown in Fig. 14 is larger than 30 m^2 of cryopump at a few degrees Kelvin.

Negative-Ion Systems - Neutral beam systems based on negative hydrogen ions will be used for acceleration and neutralization at energies above approximately 100 keV/nucleon, because of the higher neutralization efficiencies that are possible with negative ions.

Negative-ion-based beams are potentially attractive at lower energies, if suitable powers and power densities can be achieved. The advantages will be a single-energy beam, (hopefully) with fewer impurities. The same basic beamline components will be required, as for positive-ion systems. However, many of the components will be of very different design. The physics of the negative ion sources is completely different. Between the accelerator and the neutralizer there may be a strong-focussing transport section, so that most of the neutral-beam system can be outside of the radiation shielding around the fusion experiment (Fig. 15). Neutralizers may contain either gas or plasma, but the most attractive technique at present is photodetachment by a powerful laser beam.

Negative-ion-based neutral beam systems are in the early stages of development. The first applications on fusion experiments are expected to be in the mid-1990's. Present development activities on negative-ion sources is about evenly split between two production mechanisms: electron capture in a metal vapor[36,37], or production on low-work-function surfaces.[38,39] A third production technique, dissociative attachment in a discharge[40], is in the research phase and shows considerable promise.

Efficiencies - There are several types of efficiency to consider, e.g. the neutralization efficiency, and the system efficiency. From an application viewpoint, it is the system cost and the system efficiency that are of most interest. However, for the present discussion, the topic of interest is the neutralization efficiency. Calculated curves of this neutralization efficiency, defined as neutral-beam power divided by accelerated-beam power, are shown as a function of energy for several ions and neutralizers in Fig. 16. The potential advantage of negative ions, and especially a negative-ion beam

with a photodetachment neutralizer, is clear.

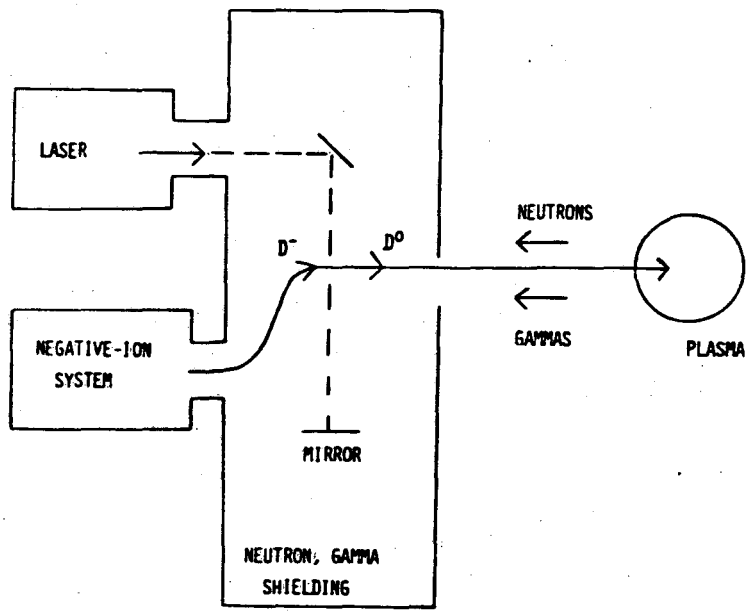

XBL 8212-12448

Fig. 15. Schematic of a negative-ion-based neutral beam system with negative-ion accelerator and neutralizer (laser components out of the line of sight for neutrons and gammas.

With one exception, no useful role has been found for molecular ion (D_2^+, D_3^+) beams, in fact, it is almost always desireable to minimize the D_2^+ and D_3^+ components from ion sources. This is because D_2^+ ions produce neutrals with half of the accelerated energy and D_3^+ ions give one-third-energy neutrals. These low-energy neutrals rarely penetrate far enough into the target plasma to do anything useful.

POSITIVE-ION BASED SYSTEMS

In this section some details of atomic physics processes in positive-ion systems will be summarized. An excellent review of this topic is given in Ref. 41; this paper contains many references which will not be repeated here. The variety of physical processes, especially in the plasma source, is large, and knowledge of the physical conditions (the electron-energy distribution, for example) is usually poor. Moreover, in most ion sources the wall interactions play a decisive role, and the physical condition of these surfaces is unknown, and perhaps unknowable. Finally, many of the phenomena are controlled as

much by plasma effects as by atomic physics. Still, progress requires at least a qualitative understanding of the physics involved.

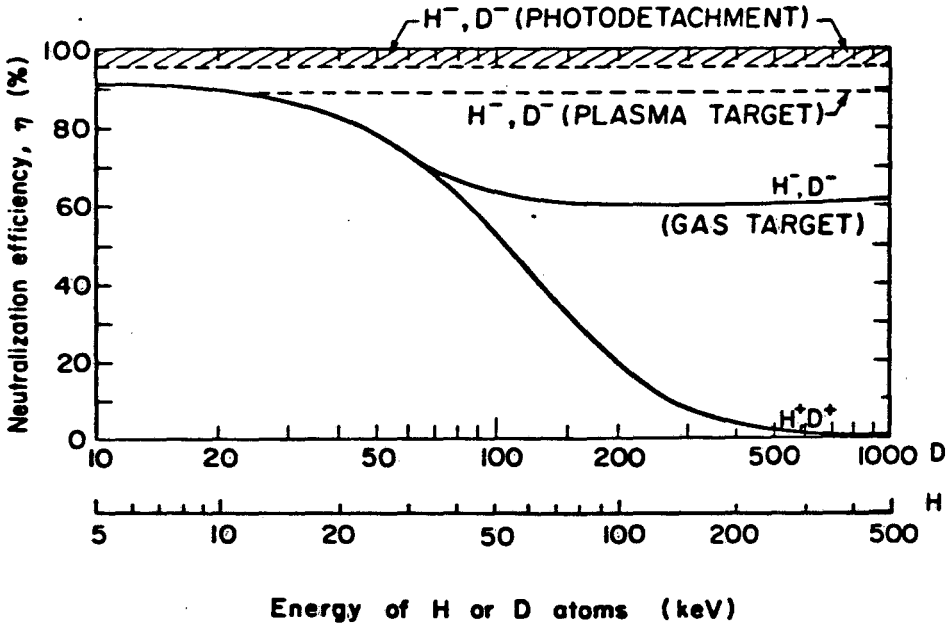

Fig. 16. Neutralization efficiencies for several ion beams and neutralizers.

ION SOURCE

Volume Atomic Processes - A list of what is believed to be the more important reactions taking place in the volume of a hydrogen plasma is given in Table 2. Cross sections for some of these are given in Figures 17a and b. Some points of special interest are the thresholds for production of H^+, H_2^+, and H_3^+ ions, because in general we want to maximize H^+ production and minimize H_2^+ and H_3^+ production, and sometimes want to maximize the H_2^*.

Impurities also are ionized by the electrons. These impurities come from the cathodes and walls of the discharge chamber, the largest component being oxygen. From an analysis of the accelerated beams, we infer that oxygen impurity ions, primarily hydride-ions, constitute several percent of the plasma under typical conditions.

Surface Atomic Processes - Atomic processes at the discharge chamber walls play an important role, and, in principle, could play a dominant role in the determination of the composition of

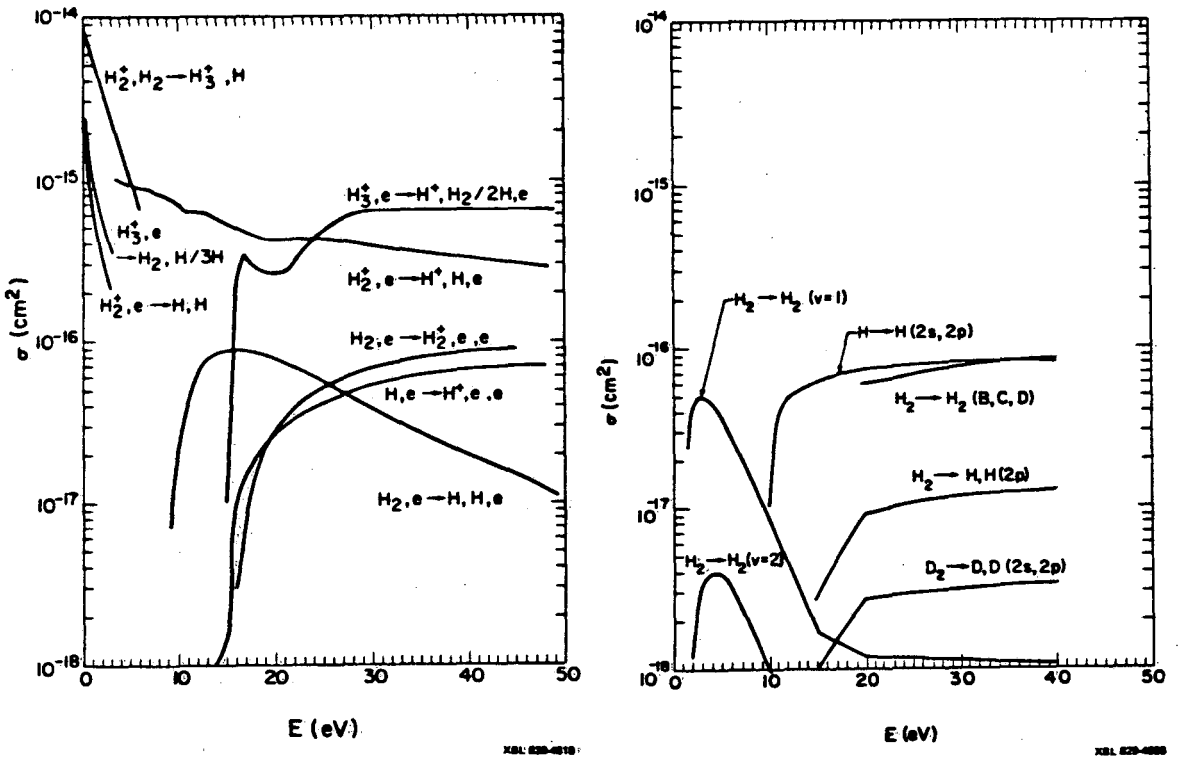

Fig. 17. Cross sections of reactions occurring in the volume of a hydrogen plasma.

the plasma. Hydrogen molecules introduced into the chamber are partially dissociated by the discharge. For the neutral hydrogen densities existing in these sources, about 10^{14} cm^{-3}, most of the atoms and molecules go to the walls without gas collisions, and then return to the volume in their original or different states. If recombination did not occur at the walls, then the neutral hydrogen atom component of the gas could be increased, and the molecular-ion fraction of the beam decreased. So far, we have not found a practical way to do this. Heating the walls to ~ 2300C is a possible, but difficult engineering approach. Oxygen found in neutral beams is assumed to come from chemical reactions between atomic hydrogen and oxides.

Source Model - We need a model of the plasma in an ion source in order to predict how to make improvements. For example, for some applications it is important that the atomic (H^+, D^+) ion percentage of the accelerated beam be 90% or greater. The properties of the discharge are strongly dependent on plasma and atomic physics in the volume and at the walls. In one model[42] cross sections for ten atomic and molecular volume processes (Fig. 17), a recombination coefficient for the walls

Table 2. Hydrogen reactions occurring in the volume of an ion-source plasma. Three types of excitation reactions are included.

$H + e \rightarrow H^+ + 2e$	$H_3^+ + e \rightarrow H^+ + H_2 + e$
	$H^+ + 2H + e$
$H_2 + e \rightarrow 2H + e$	$H_3^+ + e \rightarrow H_2 + H, 3H$
$H_2 + e \rightarrow H_2^+ + 2e$	$H_3^+ + e \rightarrow H_2 + H, + e$
$H_2^+ + e \rightarrow 2H$	$H + e \rightarrow H^*(2s,2p) + e$
$H_2^+ + e \rightarrow H^+ + H + e$	
$H_2^+ + H_2 \rightarrow H_3^+ + H$	$H_2 + e \rightarrow H_2^*(B,C,D) + e$
	$H_2 + e \rightarrow H_2^*(v=1,2,3) + e$

and a self-consistent calculation of the electron energy distribution yield D^+, D_2^+, and D_3^+ current densities at the walls. The reaction rates for the processes used are given in Fig. 18 a,b. With the model of Reference 42 it is possible to predict the ratios of H^+, H_2^+, and H_3^+ over a wide range of arc power if the wall recombination coefficient is assumed to be $\gamma = 0.2 \pm 0.1$.

Magnetic Filter - The concept of a "magnetic filter"[43] is shown in Fig. 19. High energy electrons (50-100 eV) enter the plasma from a sheath at the filaments, and would produce H^+, H_2^+ and H_3^+ ions throughout the volume if no barrier existed. The inclusion of a weak transverse magnetic field (~ 100G) prevents most of the high-energy electrons from reaching the accelerator, because they must diffuse across the "magnetic filter" and experience energy-degrading collisions in the process. The electrons near the accelerator have too low an energy to produce many molecular ions, but help destroy the molecular ions that diffuse from the filament side. In this way the H^+ fraction at the accelerator can be raised by as much as ten percentage points. There is, of course, a price: The arc

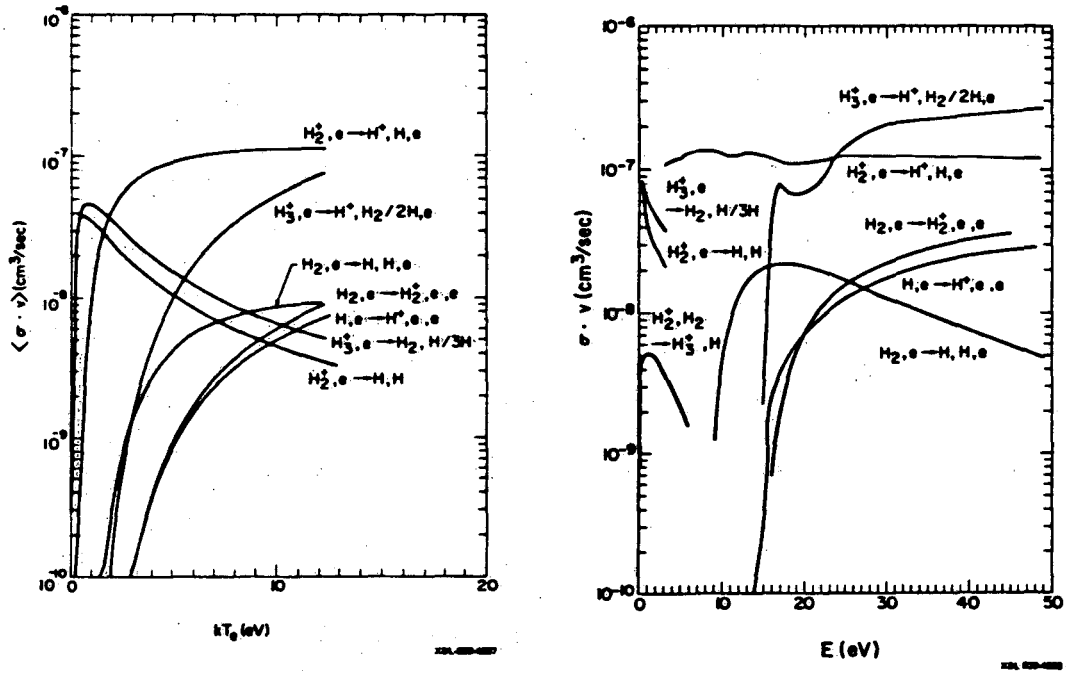

Fig. 18. Hydrogen reaction rates used in a positive-ion source model.

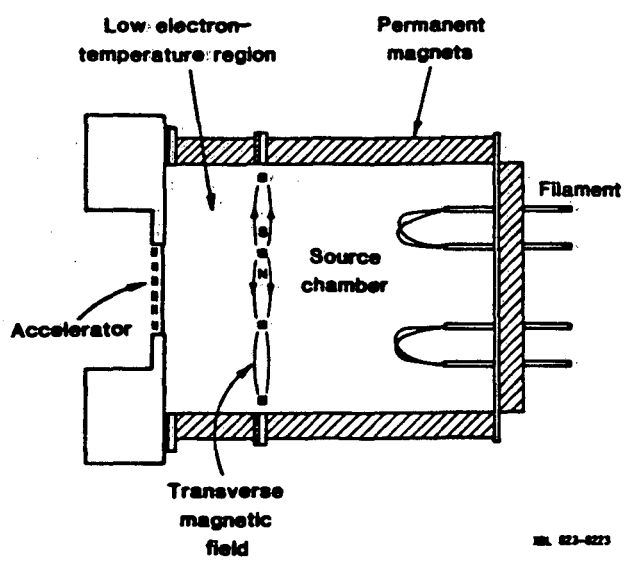

Fig. 19. "Magnetic-filter" plasma source, designed to enhance the H^+, D^+ fraction of ions later accelerated and neutralized.

power must be raised to maintain the same ion density at the accelerator.

Experimentally it was found in the first try that the electron temperature on the filament side is ~ 10 eV and the accelerator side ~6 eV; six electron volts is sufficient to produce molecular ions. The computer model shows that the optimum electron temperature is about 3 eV. At the optimum the H^+ fraction of ions in the accelerated beam is about 90%. The computer model also predicts the optimum length of the filtered plasma. i.e., the optimum distance from the filter to the accelerator.

ACCELERATOR

The atomic physics processes in the accelerator are of the same kind as given in the next section, namely ionization and charge exchange in the gas passing from the plasma source to the neutralizer. Several percent of the ions can interact with the neutral gas while being accelerated. Ion-electron collision products can be troublesome, e..g., electrons are accelerated in the backward direction and may produce x-rays or melt the ion source.

NEUTRALIZER

The neutralizer section of nearly all positive-ion-based neutral beam systems is a relatively simple mechanical device one or two meters long, with a cross section slightly larger than that of the beam from the accelerator. At the position where the beam enters it, the neutral gas streaming through the accelerator from the neutralizer has a density of about 10^{14} cm^{-3}. At the exit end of the neutralizer, the density is an order of magnitude lower. The length of the neutralizer is set by the desire to convert as much of the ion beam to neutrals as is consistent with the optical properties and cost of additional beamline.

Collisions in the neutralizer produce a plasma ($n \sim 10^9$-$10^{10} cm^{-3}$) with electron energies of several eV. The effects, if any, on the composition of the neutralizing gas have not been determined.

<u>Cross Sections</u> - In the neutralizer there is a competition between the conversion of atomic positive ions to neutrals, governed by the cross section σ_{10} (Fig. 20a) and the

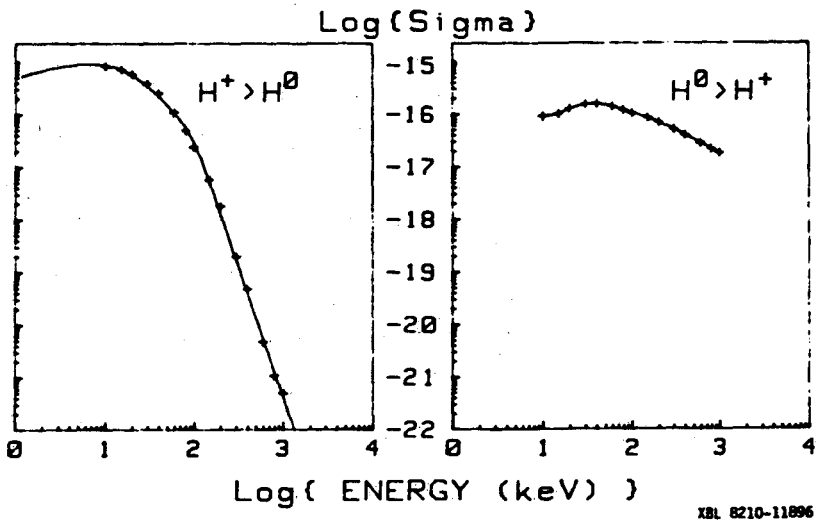

Fig. 20. Cross sections for conversion of H^+ to H^0, σ_{10}, in H_2(a) and conversion of H^0 to H^+, σ_{01}, in H_2(b).

destruction of neutrals, σ_{10}, (Fig. 20b). Usually we can ignore the cross sections for production and destruction of negative ions when calcuating the neutral yield (this is not true when one is interested in the emerging ion beams; at lower energies (~ 10 keV) approximately one percent of the accelerated positive ion beam can be converted to negative ions). Molecular ions are dissociated or neutralized before equilibrium of the high-energy component is achieved. Because actual neutralizers are not of equilibrium thicknesses, some molecular ions survive and, in fact, are useful for system diagnostics[44]. However, we do not include the cross sections here; these data can be found in compilations such as the series Atomic Data for Fusion[45].

Neutral Fractions - From a differential equation including electron capture and electron loss, we find that the neutral fraction of a beam origionally consisting of H^+ ions, after traversing a neutralizer with a "thickness" of τ molecules/cm^2, is

$$F^0 = \frac{\sigma_{10}}{\sigma_{10} + \sigma_{01}} \exp\left[1 - e^{-(\sigma_{10}+\sigma_{01})\tau}\right] ,$$

where σ_{10} and σ_{01} are electron capture and loss cross sections, and τ is the neutralizer thickness in molecules cm^{-2}. In the limit of an infinitely thick target

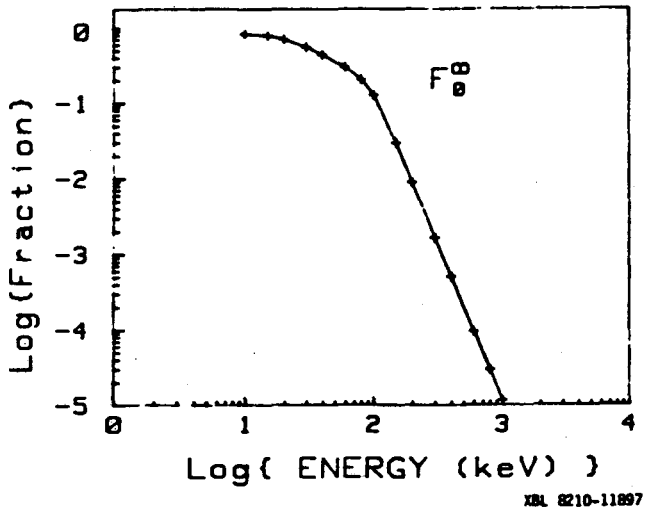

Fig. 21. The neutralization efficiency for a thick target $\sigma_{10}/(\sigma_{10} + \sigma_{01})$.

$$F_\infty^0 = \frac{\sigma_{10}}{\sigma_{10} + \sigma_{01}} .$$

F^0, obtained from the data of Fig. 20, is shown in Fig. 21. Note that the efficiency falls off approximately as E^{-4} at high energies. The approach to F_∞^0 as the neutralizer thickness is increased is shown in Fig. 22 for 80 keV/AMU ions. As a practical matter, increasing the neutralization efficiency usually means increasing the gas throughput, and hence the pumping required. As a compromise, system designers may use a neutralizer giving about 90% of F_∞^0.

Gases other than hydrogen may be used as neutralizers. Some years ago several large mirror experiments built up a confined plasma in an ultra-high vacuum by "Lorentz-ionization" of neutral beams. Beams of highly-excited atoms (magnesium vapor is a good neutralizer for producing them) were ionized by the action of the equivalent electric field $\bar{\varepsilon} = \bar{v} \times \bar{B}$ in the trapping region. In general use, however, F_∞^0 is pretty much independent of the gas used, and hydrogen is the common choice.

Region between Neutralizer and Plasma - To accomodate the ion-deflection magnet, ion-beam stops, calorimeters and duct through the coils of the confinement experiment, the beam line following the neutralizer may be six or more meters long. To prevent appreciable re-ionization of the neutral beam, the average background gas (mostly hydrogen) density must be such that $\sigma nL \ll 1$ for all neutral particles (Fig. 20b). This can be achieved by large cryopumps and careful analysis and control of

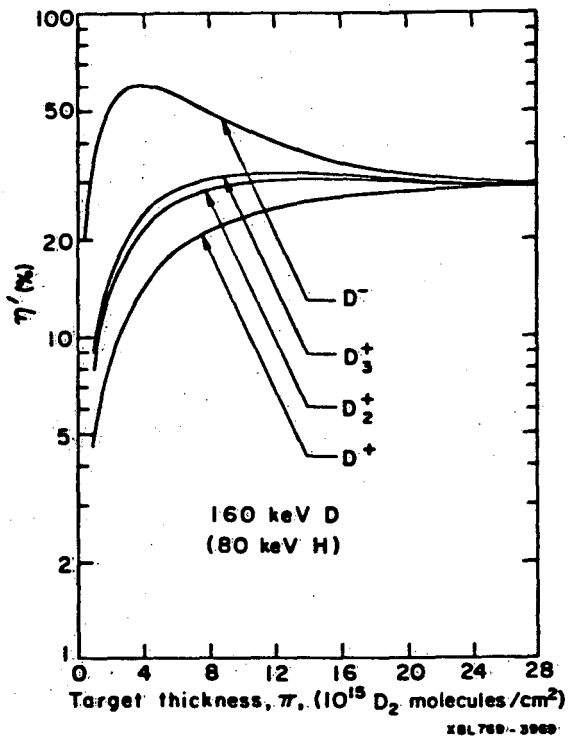

Fig. 22. The approach to equilibrium with increasing target thickness.

where stray beams strike surfaces and cause gas to be evolved.

This region presents many challenges to the engineer and to the physicist developing neutral beam diagnostics.

NEGATIVE ION BASED SYSTEMS

There is no operational high-current neutral beam system based on negative ions, and may not be for 5-15 years because the main incentive for this expensive development is a future fusion experiment not yet approved, and perhaps not yet conceived. However, the perceived need and required lead time are so great that the research and development programs around the world are growing rapidly. There are many areas requiring work by atomic and plasma physicists.

Negative-Ion Generator

Three ways to form large sources of negative hydrogen ions are currently being considered; they are, in the order in which they are being tried:

Conversion of Low-Energy Positive Ions to Negative Ions by Charge Exchange - The research described in Refs. 36 and 37 is based on the production of a high-current low-energy positive-ion beam which passes through an alkali or alkaline-earth-metal vapor, and emerges as a mixture of H^+, H^0, and H^-. The negative-ion yields that can be obtained from a thick target are quite large at low ion energies (Fig. 23),[46] as much as 50%. From a practical viewpoint, additional factors must be considered, eg. obtainable positive-ion current densities, scattering, space charge effects, etc.

The complication of the addition of a heavy-metal charge-exchange cell, and the possibility of contamination of the fusion experiment by the metal vapor, have made this negative-ion approach less attractive than the surface-production technique.

Production on Surfaces - The approaches described in Refs. 38 and 39 make use of the fairly large emission of negative ions from surfaces bombarded by low-energy ions and neutrals, especially those surfaces that have low work functons and high atomic-masses. Examples of pure alkali metal negative-ion secondary emission coefficients are given in Fig. 24.[47,48] A

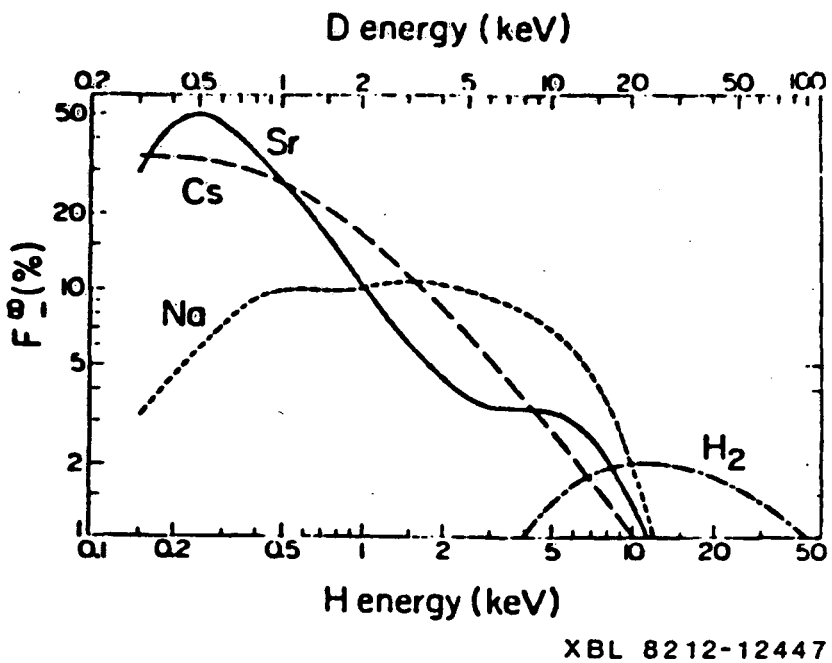

Fig. 23. The percentage conversion of H^+ to H^- in thick alkaline-earth targets.

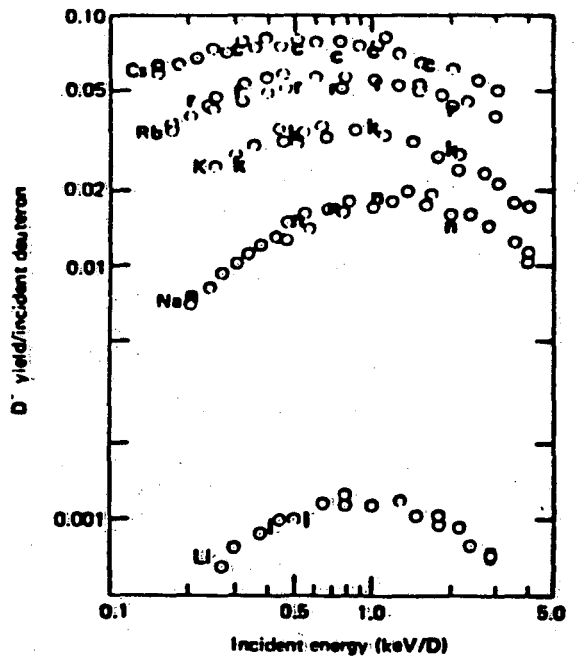

XBL 8212-12449

Fig. 24. Negative ion secondary emission coefficients for pure alkali metals.

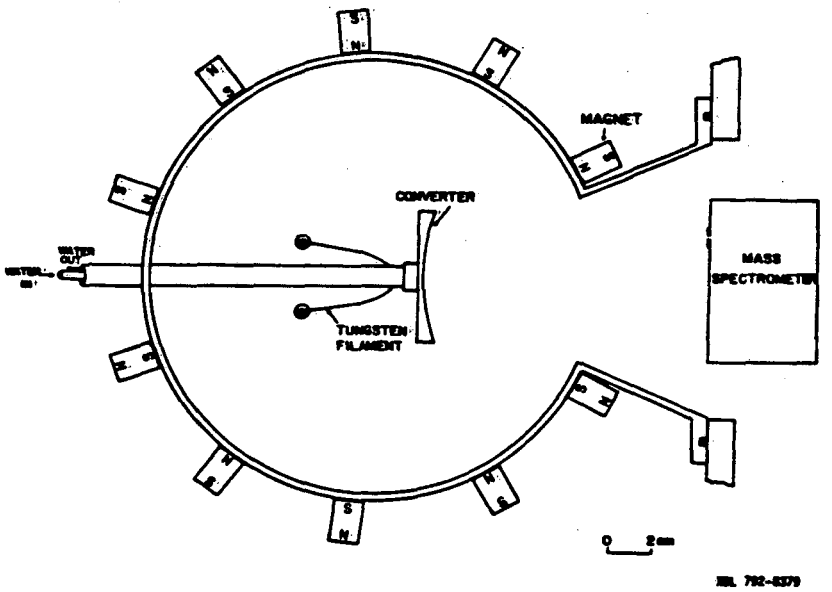

Fig. 25. Schematic of a surface-production negative ion source. The Mo "converter" is in a plasma containing hydrogen and cesium ions, and is biased positive with respect to the plasma.

model has been developed that explains these results, and those for partial coverages yielding lower work functions (for example, a partial monolayer of Cs on Mo). We also know that the H^- yield for thermal bombardment energies is rising with energy, but very low. Unfortunately, data are missing for the critical region between about 3 eV and 100 eV. From experiments with an actual ion source containing hydrogen and cesium[39] in which the energy spectra of negative ions are measured carefully, it appears that the negative ions are produced by scattering of < 10 eV neutrals, or by a different process, e.g., collisional desorption of H^- from the surface. These H^- production roles in sources consequently are still research topics.

Volume Production Charge-Exchange and Surface - The H^- production techniques require the use of cesium on other metal vapors and plasmas. We would rather not use such materials near accelerators and confinement experiments. It has been shown[40] that quite large H^- densities can exist in a plasma. (Whether currents of interest to fusion can be drawn from a volume production source, and if so, with satisfactory electron and gas control, remains to be seen.)

The proposed formation mechanism is dissociative attachment of low-energy electrons to vibrationally excited H_2 molecules:

$$e + H_2(V > 6) \rightarrow H_2^- \rightarrow H^- + H$$

This topic is discussed in Ref. 49. The production and destruction of the vibrationally-excited molecules in the plasma and at the walls is an important research topic.

Neutralizer

There are several intriguing possibilities for efficient neutralizers. The reason is that neutralization is obtained by removing a weakly-bound electron, rather than by adding an electron as in the positive ion case. The electron can be removed by collisions with gas atoms or molecules or charged particles, or by photodetachment. From Fig. 16, the neutralization efficiency is seen to be high (> 60%). It is even higher in an ionized gas, and can approach 100% in a photodetachment neutralizer. In all of these neutralization schemes the neutralization efficiency at high energies is independent of energy because the cross sections for loss of an electron from an H^- ion and from an H^0 atom have the same energy dependence.

Figure 22 shows that there is a value of the target thickness for which the neutralization efficiency is a maximum. If

we neglect cross sections other than the two-electron loss cross sections for the H^- ion and H^0 atom, σ_{-10} and σ_{01}, respectively, then

$$\varepsilon(\pi) = \frac{\sigma_{-10}}{\sigma_{01} - \sigma_{-10}} \left[e^{\frac{1}{2}\pi(\sigma_{01}-\sigma_{-10})} - e^{\frac{1}{2}\pi(\sigma_{01} - \sigma_{-10})} \right] e^{-\frac{1}{2}\pi(\sigma_{01}+\sigma_{-10})}$$

This expression has a maximum when

$$\pi = \frac{\ln(\sigma_{-10}/\sigma_{01})}{\sigma_{01} - \sigma_{-10}}$$

A more accurate result is obtained by including collisions in which two electrons are lost, with the cross section σ_{-11}. These can be included in the formula for η by replacing σ_{-10} by $\sigma_{-10} + \sigma_{-11}$ everywhere except in the numerator pf the first term. At low energies a negative ion production term must be included, but this process is negligible at energies of interest to fusion.

The practical use of lasers for photodetachment is discussed in Ref. 50. The ionization cross section peaks at a photon energy of about 1.5 eV, which is not far from the wavelength of the powerful steady-state iodine chemical lasers.

In addition to offering the possibility of approximately 100% neutralization, the photodetachment approach offers other advantages. The absence of left-over ion beams to dispose of makes the neutral beam system much simpler and cheaper. Moreover, the photoionization process is selective, so that impurities may be eliminated from the neutral beam.

DIAGNOSTICS

Good diagnostics of physical conditions in various parts of the neutral beam line is important in the research and development phase, and in the operations phase. Because power densities in present neutral beams are tens of kilowatts per square centimeter, and pulses are > 1 S, it is difficult or impossible to sample the neutral beams for composition or impurities with solid analyzers, especially when the beams are being injected into the plasma targets. Techniques are in use, or need to be developed, which utilize natural emission from the beam, or non-perturbing optical or particle probes.

The most important neutral beam properties are the currents and angular distributions of the full-, half-, and one-third-

energy hydrogen or deuterium atoms that reach the plasma, and the currents of neutral impurities. No good techniques for measuring impurity currents have been developed, and the very useful doppler-shift optical technique measurements (described next) are made in the neutralizer rather than at the exit end of the beam line. We expect laser techniques to provide powerful diagnostic aids in coming years.

Doppler-Shifted Light--The energy and spatial distributions of a neutral beam can be measured by observing the doppler-shifted Hα and Hβ light emitted by the beam as it transverses the neutralizers.[51,52] Accelerated H^+, H_2^+, H_3^+ ions interact with the gas in the neutralizer and produce atoms with energies E, 1/2E, and 1/3E, where E is the final energy of the accelerated ion beam. By observing the radiation emitted by the beam at an angle to the beam direction, three separate Doppler-shifted spectra can be recorded.

To obtain neutral currents, it is necessary to know the following cross sections (others turn out to be unimportant for usual conditions).

1. $H^+ + H_2 \rightarrow H^*$ (3S, 3P, and 3D levels)
2. $H^o + H_2 \rightarrow H^*$ (")
3. $H_2^+ + H_2 \rightarrow H^*$ (")
4. $H_2^o + H_2 \rightarrow H^*$ (")
5. $H_3^+ + H_2 \rightarrow H^*$ (")
6. $H_2^+ + e \rightarrow H^*$ (3s) + H(1S) or H^+

The light intensity of the ith component (i = 1, 2, 3, corresponding to full, half, and third energy) is proportional to N(n), (the population density of the nth level of excited hydrogen atoms with velocity v_i). Using an index j to refer to species considered in this model

$$N(n)_i = \frac{1}{v_i} \sum_j n_o(z - x)\, \sigma_j(n)\, J_j(x) \exp\left(-\frac{x}{v_i T_n}\right) d_x,$$

where v_i is the velocity of the ith component, z is the distance between the observation point and the exit grid of the source, n_o is the density of the gas in the neutralizer, $\sigma_j(n)$ is the optical excitation cross section for the jth species in the mixed beam $J_j(x)$ is the current density of the corresponding species, T_n is the lifetime of the nth level of hydrogen, and j is summed over those species contributing to the

ith component of the beam.

The data are processed by a computer to yield (1) the neutral currents (from the areas under the curves), (2) the angular distribution for each energy fraction (from the widths of the peaks), and (3) the mean directions of the neutral beams (from the centroids of the peaks).

A signal corresponding to a hydrogen atom energy of about E/18 is believed to be from the breakup of accelerated water ions, and hence gives a measure of the oxygen impurity in the neutral beam.

Special Topics

Ideas for beams different from those discussed so far ie, the conventional neutral H or D beams, have arisen recently. One of them, the use of intense tritium beams, does not change the atomic physics appreciably, but will present new engineering problems. Some other suggestions are

1. "Light" atoms, e.g., Li through Ne; the application of such beams has been discussed in Section II of this article.
2. Polarized neutral beams.

Polarized Neutral Beams--One of the most intriguing ideas is to inject polarized neutral beams into a polarized plasma. Both the nuclear reaction rates and the angular distributions of the reaction products could be favorably modified.[53] Several ways for obtaining nuclear polarization in conventional polarized ion sources are given in Ref.[54] Whether these, or other techniques, can be applied to intense neutral beam systems remains to be seen.

ACKNOWLEDGMENTS

The authors are grateful for discussions with and assistance from Drs. D. Mikkelsen, C. Singer, L. Grisham, R. Goldston, and K. Berkner, F. Burrell, W. S. Cooper, K. Ehlers, K. N. Leung, and Mr. J. W. Stearns.

This work was supported by in part by the Director, Office of Energy Research, Office of Fusion Energy, Development and Technology Division, of the U.S. Department of Energy under Contract No. DE-AC03-76-SF00098, and in part by PPPL DOE Contract No. DE-AC02-76-CH03073.

REFERENCES

1. J. D. Lawson, Proc. Phys. Soc., London, Sect. B 70, 6 (1957).
2. S. Greene, 1967, UCRL-702522, Lawrence Livermore Laboratory, Livermore, California.
3. T. Ohkawa, Nucl. Fus. 10, 85 (1970).
4. T. K. Fowler, "Mirror Theory", Fusion, Vol. 1, ed. E. Teller, Academic Press (1981).
5. R. F. Post, "Experimental Base of Mirror Confinement Physics, Fusion, Vol. 1, ed. E. Teller, Academic Press (1981).
6. H. Furth, "The Tokamak," Fusion, Vol. 1, ed. E. Teller, Academic Press (1981).
7. J. Shohet, "Stellerators," Fusion, Vol. 1, ed. E. Teller, Academic Press (1981).
8. R. Hulse, D. Post, D. Mikkelsen, J. Phys. B 13, 895 (1980) V. Krupin, V. Marchemko, and S. Kakovlenko, JETP Lett. 29, 3895 (1979).
9. W. Kunkel, "Neutral Beam Injection," Fusion, Vol. 1, ed. E. Teller, Academic Press (1981).
10. R. Freeman and E. Jones, CLM R-137, Culham Laboratory, Abingdon, England (1974).
11. J. Rome, J. Callen, and J. Clarke, Nucl. Fus. 14, 141 (1974).12.G. Lister, D. Post, and R. Goldston, Symp. Plasma Heat. in Toroidal Devices, 3rd (ed. E. Sindoni) p. 303, E'ditvice, Compositori, 1976.
13. L. D. Stewart, et al. "Proc. of 2nd International Symposium on the Production and Neutralization of Negative Hydrogen Ions and Beams," T. Sluyters, ed. BNL-51304, 1980.
14. R. Olson, K. Berkner, W. Graham, R. Pyle, A. Schlachter, and J. Stearns, Phys. Rev. Lett. 41, 163 (1978).
15. H.B. Gilbody, Physica Scripta 23, 143 (1980).
16. INTOR Group, Rep. Int. Tokamak Reactor Workshop, (IAEA, Vienna) 1980.
17. M. Menon, Proc. of IEEE 69, 1012 (1981).
18. J.A. Holmes, J. Rome, W. Houlberg, Y-K. Peng, and S. Lynch, Nucl. Fus. 20, 59 (1980).

19. T. Stix, Plasma Physics 14, 367 (1972).
20. D. Sivukhin, in "Reviews of Plasma Physics," (M.A. Leontovich, ed.) Vol. 4, Pergammon, Oxford (1966).
21. H. Eubank, et al., Phys. Rev. Lett. 43, 270 (1979).
22. J. Dawson, H. Furth, and F. Tenney, Phys. Rev. Letter 26, 1157 (1971).
23. R.C. Isler, C. Crume, Phys. Rev. Lett. 41, 1296 (1978).
24. S. Suchever, E. Hinnov, M. Bitter, R. Hulse, D. Post, Phys. Rev. A (to be published).
25. W. Clark, J. Cordey, M. Cox, S. Fielding, R. Gill, R. Hulse, P. Johnson, J. Paul, W. Peacock, B. Powell, M. Stamp, and D. Start, Nucl. Fusion 22, 333.
26. D. Mikkelsen and C. Singer, "Optimization of Steady-State Beam-Driven Tokamak Reactors," (to be published).
27. W. Clark, J. Cordey, M. Cox, R. Gill. J. Hugill, J. Paul, and D. Start, Phys. Rev. Lett. 45, 1101 (1980).
28. S. Suchewer, et al., Phys. Rev. Lett. 43, 207 (1979).
29. L. Grisham, D. Post, D. Mikkelsen, and H. Eubank, Nuclear Technology/Fusion 2, 199 (1982).
30. J. Dawson and K. MacKenzie, Proceedings of the 2nd Joint Grenoble-Varenna International Symposium, EUR-742-EN, p. 953 (1980).
31. M. Gryzinski, Phys. Rev. Lett. 138, A336 (1965).
32. K. H. Berkner et.al., Proc. 8th Symp. Engin. Prob. Fusion Research, San Francisco, IEEE Pub. Mo. 79 CH 1441-5NPS (1979) p. 214.
33. W. Gardner, et.al., RSI 53, 424 (1982).
34. P. Reardon, "Status Report on TFTR", Proc. 3rd Topical Meeting on the Technology of Nuclear Fusion, Santa Fe (1978) p. 621.
35. K. H. Berkner, et.al. Proc. 9th Symp. Engin. Prob. Fusion Research, Chicago IEEE Pub. No. 81CH1715-2NPS (1981) p. 763.
36. E. B. Hooper, P. Poulsen, P. Pincosy, JAP 52 7027 (1981); E. B. Hooper, P. Poulsen, O. A. Anderson, Nucl. Tech. Fusion 2, 362 (1982).
37. M. Delannay, et al. "A New Type of Neutral Injector Based on the Production of D^- by Double Elextron Capture," Heating in Toroidal Plasmas, Proceeding of the 2nd International Symp., Como, Italy, Sept. 1980, p. 831.
38. Yu I. Belchenko and V. G. Dudnikov, Proc. of the 15th Intl. Conf. on Phenomena in Ionized GAses, Minsk (1981) p. 1504.39. K. N. Leung and K. W. Ehlers, RSI 53, 803 (1982).
40. G. W. Hamilton and "Proceedings of the Second Intl. Symp. onProduction and Neutralization of Negative Hydrogen Ions and Beams, Brookhaven Natl. Lab. (1980) p. 90.
41. P. Raimbault and J. P. Girard, "Atomic and Molecular Physics Problems in Fast Neutral Injection," Physica Scripta 23, 108 (1982).
42. C. F. Burrell, C. F. Chan and W. S. Cooper (LBL), private communication.

43. K. W. Ehlers and K. N. Leung "Effect of a Magnetic Filter on Hydrogen Ion Species in a Multicusp Ion Source. LBL Report (LBL-12255) (1981).
44. J. W. Stearns, private communication.
45. D. H. Crandall and C. F. Barnett (ORNL) and W. L. Wiese (NBS)"Atomic Data for Fusion," Controlled Fusion Atomic Data Center, ORNL.
46. R. McFarland, A. S. Schlachter, J.W. Stearns, R. Olson, "D^- Production by Charge Transfer in Thick Alkaline-Earth Targets," to be published in Physical Review A.
47. P. J. Schneider, et al., Phys. Rev. B 23, 941 (1981).
48. J. R. Hiskes, P. J. Schneider, Phys. Rev. B 23, 949 (1981).
49. J. R. Hiskes, et al., "Hydrogen Vibrational Population Distributions and Negative Ion Concentrations in a Medium Density Hydrogen Discharge, "Lawrence Liverore National Laboratory Report UCRL-86873 (1981).
50. J. H. Fink, "Evaluating Laser-Neutralized Negative Ions as a Source of Neutral Beams for Magnetic Fusion Reactors," Lawrence Livermore National Laboratory Report UCRL-87301 (1982).
51. C. F. Burrell, et al., "Doppler Shift Spectroscopy of Powerful Neutral Beams, RSI 51, 1451 (1980).
52. G. A. Cottrell, A. R. Martin, and C. Padget "Optical Diagnosis of a High-Current Beam," Heating in Toroidal Plasmas (1980) p. 945.
53. R. M. Kulsrud, et al. "Fusion Reactor Plasmas with Polarized Nuclei," submitted to Phys. Rev. Lett.
54 A. D. Krish and A. T. M. Lin, Editors, Polarized Proton Ion Sources, American Institute of Physics, New York, (1982).

This report was done with support from the Department of Energy. Any conclusions or opinions expressed in this report represent solely those of the author(s) and not necessarily those of The Regents of the University of California, the Lawrence Berkeley Laboratory or the Department of Energy.

Reference to a company or product name does not imply approval or recommendation of the product by the University of California or the U.S. Department of Energy to the exclusion of others that may be suitable.

TECHNICAL INFORMATION DEPARTMENT
LAWRENCE BERKELEY LABORATORY
UNIVERSITY OF CALIFORNIA
BERKELEY, CALIFORNIA 94720